IPRO 323

Modeling of Building Integrated Wind Turbine Modules

TABLE OF CONTENTS

1. Executive Summary

The purpose of wind power as a renewable energy source is to replace diminishing energy sources which have negative effects on the environment. Wind power is becoming increasingly popular as the threat of global warming and pollution looms over the world. Because the majority of energy consumption occurs in cities, the goal of IPRO 323 is to develop a methodology for designing and developing building-integrated wind turbine modules so that more urban environments will begin to use wind power as a viable energy source as an alternative to harmful and wasteful sources such as fossil fuels.

2. Purpose and Objectives

Fossil fuels have become the foundation of our energy needs. A study done in 2007 showed that fossil fuels constituted 86.4% of the primary energy consumption in the world [1]. Other non-fossil fuel sources used in 2006 included hydroelectric (6.3%), nuclear (8.5%), and other renewable sources (0.9%). World energy consumption is growing at about 2.3% annually [2]. The world's supply of fossil fuels will one day be unable to meet our energy needs.

There are also many environmental concerns about the use of fossil fuels. The effects of using fossil fuels to produce electricity include global warming and pollution. The burning of fossil fuels produces roughly 21.3 billion tons of carbon dioxide (CO_2) per year. Carbon dioxide is one of the greenhouse gases that contributes to global warming [3].

Renewable energy provides a solution to the concerns of a dwindling fossil fuel supply and environmental effects. Renewable energy sources include wind, water, solar, biomass, and geothermal energy. Renewable energy is often termed as clean energy because it uses the Earth's natural resources to produce energy. Renewable energy is a rapidly growing industry; wind power is growing at the rate of 30% annually, producing a worldwide 158 gigawatts of power in 2009 [4].

Urban environments currently use over 66% of the world's energy. In the US, buildings represent 50% of the total national energy consumption and 77% of electricity use. It is also important to mention that 30% of energy production and 67.5% of all electrical energy is lost with current infrastructure, deeming them inefficient and wasteful [5]. Studies indicate that urbanization causes an increase in CO_2 emissions as countries shift from using CO_2-neutral energy sources to CO_2-intensive energy sources in urban areas [6]. In addition to this, projections indicate that cities are likely to increase their share in global energy consumption to 73% by 2030 and 87% in the U.S. alone [7].

Being able to adapt cities to include onsite renewable technologies is of vital importance. IPRO 323 hopes to design a device that will reduce the reliance on fossil fuels in urban areas. This device will unite wind energy and high-rise buildings. Building-integratedwind turbine technology is not commonly used at the moment and research and development is required. The goal of IPRO 323 is to effectively integrate wind turbines and buildings with harmony as to not disturb the social and natural environments of the city, and to produce the maximum amount of power possible. This can be done by designing a surface shape to integrate onto buildings that will accelerate the velocity, and thus increase the power output of the wind turbines implemented on the shapes. In IPRO 323, it is not only important to understand the fluid dynamics of wind flow and energy to increase turbine efficiency, but to understand how it can be applied to urban environments and integrated onto current buildings to create architecturally efficient and aesthetically pleasing building-integrated wind turbine modules.

3. Organization and Approach

The team was divided into several subdivisions in order to achieve the IPRO 323 goals. These subdivisions included research and development, wind tunnel testing, computational fluid dynamics, and architectural analysis. The research team investigated the best methods for beginning the experimental research, and applied this to the development of the prototype and testing components. The wind tunnel team was responsible for applying research to conduct experiments and master the equipment, as well as to analyze the data gathered and make sure it made sense. The computational fluid dynamics team was in charge of predicting and verifying

the collected experimental data from the wind tunnel testing. The architectural analysis team was responsible for determining whether the theoretical power output measurements were viable for an urban high-rise building as well as determining how the finished product would be integrated into the structure in the most efficient way.

The research team read through a number of articles in order to determine the best method for beginning experimentation. Through research, it was decided that in order to better understand the optimization of wind turbine, a two-dimensional analysis should be conducted. Because of the time and cost limitations for IPRO 323 this semester, it was obvious that creating a real turbine and calculating the actual power output of the turbine would not be practical. A porous plate was chosen to model a wind turbine; an idea taken from the article "Experimental study on the wind turbine wake meandering with the help of a non-rotating simplified model and of a rotating model" by S. Aubrun, S. Loyer, and G. Espana from AIAA [8]. This AIAA study tested a 3-blade wind turbine and a porous disc with the same cross sectional area to find that the wake characteristics of each were nearly identical. The idea behind this 'mock turbine' is that it acts as a drag source and creates a pressure drop across the porous plate as compared with the pressure drop across a turbine. The article helps to verify that a mesh plate with certain porosity can imitate a wind turbine, even considering the rotational effects of the turbine blades in the wake.

The research team also helped in creating a testing method for the wind tunnel testing team by researching the fluid mechanics behind wind turbines, and the mechanisms that have previously been used to optimize the power output produced. The most useful findings came from articles on Betz' limit, and an article describing the wake characteristics of perforated plates in more depth. This helped the research team to combine with the testing and data analysis team to figure out the testing set-up for the perforated plate, the design for the surface mount prototype, and all of the measurements that would be needed in order to prove that the plate could be used to simulate a turbine, and that the prototype for the shape produced a jump in power output.

After the research team concluded that a perforated plate would suffice to simulate the wake characteristics of a wind turbine with a similar cross-sectional area, they also did literary review on flow guiding structures before determining that the first surface design prototype would be of a Gaussian shape, or bell-curve (Refer to Appendix F: Surface Design Prototype). They

determined that the most important measurements to take would be of the velocity and pressures at different locations in front of and behind the plate. Measurements of velocity and pressure would allow the data analysis to be done to determine the fluid dynamic effects of the shape and plate, and ultimately to calculate the power output of the wind turbine module simulation.

The wind tunnel testing team was responsible for conducting all experimental research. While the research team figured out what must be developed and measured, the testing team figured out what equipment was necessary, how to use the equipment, and where to take measurements to obtain enough data. The equipment also required calibration to ensure accurate measurements before any data was taken. In order to keep this analysis two-dimensional, the wind tunnel team had to figure out how to mount the perforated plate into the wind tunnel such that the plate spanned across the width of the tunnel and that the test space was clear of any obstructions that may interfere with the data collection. The biggest challenge facing the testing team was malfunctioning equipment and data that did not make sense. It was both the testing and research team's responsibility to find out why the results did not turn out as predicted, and to fix the problem and retest.

The most important measurements taken by the testing team included the wake velocities of the perforated plate to verify its similarity to the wake effects of an ideal wind turbine, the pressure drop across the perforated plate alone, the velocity difference across the surface of the prototype, and the pressure drop across the perforated plate including the shape. These results helped the research and testing teams become acquainted with a testing methodology that could be used for future work in testing different prototype shapes and possibly testing a real wind turbine integrated onto the best surface mount shape.

The Computational Fluid Dynamics team coincided with the wind tunnel testing team because they used a computer program to create a model of the wind tunnel, shape, and perforated plate to computationally analyze the fluid flow in the wind tunnel and complement the analyzed data from the testing team. Computational Fluid Dynamics (CFD) is a branch of fluid mechanics that uses numerical methods to analyze fluid flow. For this project, the CFD team was responsible constructing a valid computational model of the experiment that uses the proper differential equations to describe the motion of the fluid.

The architectural analysis team had two major responsibilities involving the end product of this semester's IPRO, as well as becoming acquainted with the fluid dynamics research and wind tunnel testing aspect of their original idea to design buildings to incorporate wind turbines. The first was to design a structure integrating the wind turbine in such a way as to not disrupt the harmony of the social and environmental atmosphere of the city. It was important for the architects to consider the material used to create the surface design, noise, bird interference, and safety. The design must also space these turbines in such a way that the wind velocity has time to recover before entering the next wind turbine. With all of these things in mind, they were able to design several three-dimensional renderings of possible ways the wind turbine module could be incorporated in typical urban buildings.

The second goal of the architectural analysis team was to gather information in regards to energy and power consumption of an average high-rise office building, and to relate these to the power output of the wind turbine module designed by the engineers. They were compared to the theoretical power output calculated from the experimental data in order to determine whether the proposed turbine design would be viable. More analysis was done on the areas and perimeters of different high rise buildings, and how the surface areas could be enhanced so that the optimum amount of wind turbine modules could be incorporated on the sides of these buildings.

4. Analysis and Findings

The perforated plate was the first component to be tested. Velocity measurements were taken at various locations behind the plate and vertically, above, below and in the middle of the plate. Because the objective was to create a plate with the characteristics to produce wake effects so that the lowest velocity behind the plate was approximately one-third of the free-stream velocity, testing was done until the velocity profile showed a low point at this value.

Once this result was found and verified with repeated tests, the pressure drop across the plate had to be measured. After verifying that this plate could be used as a wind turbine simulation, the theoretical power output for just the 'turbine' had to be calculated and later compared to the power output including the surface design. The power output for just the plate did not necessarily matter at this stage, because it would only be calculated to verify that the same 'turbine' mounted on a curved shape would produce a higher output than solely the turbine.

After the surface design was created, the velocity change had to be tested to verify that the shape would accelerate the air flow and create higher speeds at the top. These results showed a very noticeable increase in velocity at the top of the shape, so the next step was to mount the plate to the surface design and measure the pressure drop across the plate at plate locations at the top of the shape, ¾ inches, one inch, and five inches behind the top of the shape. Comparing these results to the results from the plate alone, the power output dramatically increased, with the highest power output being at the plate location five inches behind the center.

Refer to Appendix I for raw data, graphs, and full analysis.

5. Conclusion and Recommendations

This semester, an enormous amount of work has gone into researching and developing a testing methodology for IPRO 323. The semester's goal was to design and test a basic wind turbine module that could be integrated onto current buildings to optimize the power that the turbine generates. The data gathered showed satisfactory results, but there is still work to be done in order to make the concept of building-integrated wind turbine modules a reality.

The continuing research should verify results obtained this semester by repeating a power production test. From there, the wind tunnel research should build on what has been accomplished this semester. Initially, this can be accomplished by testing the existing building surface treatment with the existing perforated plate at more locations downstream and upstream of the treatment centerline to verify the location where maximum power generation could occur. Additionally, there should be tests carried out across a greater range of vertical positions away from the vertical treatment. From there, in concert with results obtained from computational fluid dynamics analysis, surface treatments with different geometries could be tested. It would be interesting to determine if the peak potential power production occurs at the same streamwise and vertical locations for different treatment geometries, or if the locations vary in some predictable manner.

In order to increase the accuracy of the power production estimations, future IPROs could implement hot wire anemometry techniques and/or force transducer measurement techniques. In all of the testing done to date, the flow has been assumed to be 2-D and perpendicular to the

treatment and porous plate, however in the real world this is an unrealistic simplification as flow geometries are highly three dimensional with the average flow direction changing on a fairly continuous basis. As a result future testing should be accomplished with models that will allow for three-dimensional effects and tested at non-perpendicular angles to the incoming flow. Future IPROs should do additional scaling effects literature research to verify the applicability of scales used during these experimental and computational studies. One other limitation presented by the wind tunnel test section currently being used for experimental testing is velocities limited to ~ 3 m/s while real world flows could be up to 5 times this. If the model is scaled down further it would potentially be possible to use the higher speed test section in the Mark V. Morkovin wind tunnel so as to test results at higher velocities.

There is also future work to be done in architectural development. It is important to note that there is much analysis to be done to implement these structures onto buildings to create aesthetically pleasing facades, to reduce costs of integration, and to implement the turbines with as little disturbances as possible in the busy urban environments they will be designed for.

With renewable energy becoming an increasingly desirable source, wind power is among the most sought after technologies at present. The development of wind turbines in rural areas has been steadily increasing in the past decades, but the overall goal of IPRO 323 is to develop a way to integrate efficient wind turbines into an urban environment where energy is most heavily consumed. With the help of engineers, architects, and industrialists, wind energy in large cities will become a common technology.

[1]"U.S. EIA International Energy Statistics". Retrieved 2010-01-12.

[2] "International Energy Annual 2006". Retrieved 2009-02-08.

[3] "US Department of Energy on greenhouse gases". Retrieved 2007-09-09.

[4] Lars Kroldrup. Gains in Global Wind Capacity Reported*Green Inc.*, February 15, 2010.

[5] http://www.architecture2030.org/

[6] http://www.worldfuturecouncil.org/fileadmin/user_upload/papers/WFC_Regenerative_Cities_web_final.pdf

[7] http://www.oecd.org/home/0,2987,en_2649_201185_1_1_1_1_1,00.html

[8] http://www.wind-power-program.com/betz.htm,"Experimental study on the wind turbine wake meandering with the help of a non-rotating simplified model and of a rotating model" by S. Aubrun, S. Loyer and G. Espana from AIAA

[9] Betz, A. (1966) *Introduction to the Theory of Flow Machines.* (D. G. Randall, Trans.) Oxford: Pergamon Press.

[10] "Wake Characteristics of two-dimensional perforated plates normal to an airstream" by Castro

APPENDICES

PART 1: STRUCTURE

Appendix A

List of Team Members

Jose Luis Amodio Leon
Corey Bushcott
Edward Ciciora
Taylor Dizon
Antonio Gonnella
Kent Hoffman
Nyla Husain
Thiago Jardim
Jaeyoung Kim
Tom McManus
Lucas Pfiffner
Jonathan Swanson
Dr. Wark
Dr. Rempfer

Sub-Teams

Research and Literary Review
Wind Tunnel Testing and Data Analysis
Computational Fluid Dynamics
Architectural Research and Development

Appendix B

Semester Budget

Expense Category	-	Amount		Percent of Total
Equipment	**$**	0		0.00%
Materials and Supplies	**$**	1,500		65.79%
Publications and Communications	**$**	180		7.89%
Travel Expenses	**$**	0		0.00%

Prototyping	**$**	500		21.93%
Other Expenses	**$**	100		4.39%
Total	**$**	2,280		**100.00%**

Table 1: IPRO 323 Semester Budget

Materials and Supplies

A major component of this IPRO was wind tunnel testing and as such there were several items that needed to be purchased for the construction of the model as well as the testing of the model. The materials & supplies that were needed to perform the wind tunnel tests included foam (to make the façade), glue, tape, goo-gone/degreaser/solvent, MDF (for the façade template), tape (scotch super 88), wire (for cutting the façade), perforated plate for modeling the wind turbine and miscellaneous parts to secure, position and provide ease of movement of the models in the tunnel, such as clamps and rods. The planform of the test section in the wind tunnel is four feet wide and approximately five feet in length, so the single biggest expense in this category was the purchase of relative large pieces of good quality foam.

Publications and Communications

Some funding was required for publishing the data and findings. The budget for this portion of the IPRO went to the cost of purchasing and printing posters and brochures for the final presentation of the team's goals and accomplishments.

Prototyping

Additional funding was needed for the prototyping of the test shape for the wind tunnel. It was expected that several prototypes would be made for the testing in the wind tunnel; this budget was used to ensure adequate funding for this purpose.

Other Expenses

A budget for other expenses was limited to $100 for team recreation, food, and beverages.

PART 2: RESEARCH AND DEVELOPMENT

Appendix C

Energy Sustainability and Wind Power

To reverse the collision course between humans and nature is the primary challenge of our time. As global climate change and population growth increases, human footprint exceeds the world's biological capacity. It is imperative to mitigate and offset Green House Gases emissions by changing the current energy supply source in order to minimize such conflict. It is also important to address the inefficiency of current energy transmission systems and integrate innovative technology such as smart grids and on-site renewable energy generation.

One of the most important locations of energy consumption is in urban environments: "Modern cities are defined by the concentration of economic activities and intense human interaction… The ravenous appetite of our cities' fossil-fuel powered lifestyles for resources from the world's ecosystems has severe consequences for all life on Earth, including human life" (World Future Council; Regenerative Cities Report published at the COP 16, Cancun). Cities are responsible for the enlargement of the global population and increase in economic and social development and the unsustainable transformation of vast amounts of natural capital to physical and social capital. "As countries urbanize, they tend to shift from CO_2-neutral energy sources (biomass and waste) to CO_2-intensive energy sources, leading to an increasing proportion of carbon dioxide emissions from cities (Jollands in OECD, 2008a). Cities and towns currently use over two-thirds of the world's energy although they only account for approximately 50% of the world's population. Projections indicate that cities are likely to increase their share in the total world energy consumption. By 2030, cities are expected to account for more than 60% of the world'spopulation and 73% of the world's energy use. US cities will likely account for 87% of US energy consumption in 2030, compared with 80% in 2006." (OECD) In the US, the building industry is powered mainly from coal and natural gas. Buildings represent 50% of the total energy consumption, 77% of the total electricity use, and emit a share of 38% of the national GHG emissions. It is also important to add that 30% of all energy production and 67.5% of all electrical energy is lost with current infrastructure (EIA / Architecture 2030).

Thus far, being able to adapt cities to include on site renewable technologies is of vital importance for the health of the global environment. New technologies must be developed to optimize the sustainable energy created by power sources such as solar panels and wind

turbines.The IPRO 323 group has had the opportunity to address this challenge by analyzing surface designs for building integrated wind turbines. Testing and analysis of a curved building shape for optimum wind speed and power output were used to in attempt to achieve a more efficient solution to increase wind energy in urban environments.

Sources:

http://www.worldfuturecouncil.org/fileadmin/user_upload/papers/WFC_Regenerative_Cities_web_final.pdf
http://www.architecture2030.org
http://www.architecture2030.org/enews/news_032911.html
http://www1.eere.energy.gov/ba/pba/intensityindicators/trend_definitions.html
http://buildingsdatabook.eren.doe.gov/default.aspx

Appendix D

Power Consumption in Urban Environments

The following is a table of typical power consumption values for common building types in city and town environments:

			Consumption (kWh)		Cost
		Tot. (bn kWh)	Avg/Bldg	Avg/SqFt	Dollars/100kWh
Office Buildings		**198**	**281**	**18.9**	**$7.08**
	Small	16	39	14.8	$8.29
	Medium	58	223	15.4	$8.06
	Large	124	3252	22.1	$6.46
Health Care		**62**	**589**	**26.5**	**$6.31**
Type	Inpatient	49	2242	30.1	$5.91
	Outpatient	12	151	18.1	$7.88
Size	Medium	10	247	18.0	$7.02
	Large	49	6,886	30.3	$5.93
Education		**65**	**210**	**8.4**	**$7.99**
	Small	4	38	15.0	$9.46
	Medium	27	158	8.2	$8.51
	Large	34	894	8.2	$7.42

Retail /Service		**149**	**117**	**11.8**	**$7.83**
Type	Retail	105	151	11.6	$7.84
	All Malls	61	429	12.9	$7.64
	Strip Malls	39	298	13.4	$7.94
	Enclosed	22	1833	12.3	$7.10
	Other Retail	44	80	10.1	$8.12
	Service	44	76	12.3	$7.82
Size	Small	26	36	14.4	$8.76
	Medium	59	115	9.4	$8.39
	Large	64	2146	14.0	$6.93
Food Service		**49**	**171**	**36.0**	**$8.07**
	Small	31	147	56.3	$8.64
	Medium	17	229	22.1	$7.12

Table 2: Typical power consumption for buildings in an urban environment.

Small = 1,001 to 5,000 Sq Ft
Medium = 5,001 to 50,000 Sq Ft
Large = >50,000 Sq Ft

Sources:
Energy Information Administration, 1995 Buildings Energy Consumption Survey.

Appendix E

Betz' Law: Wind Energy Limit

A wind turbine's ideal efficiency can be derived using Betz' Law. By analyzing the fluid dynamics through an 'actuator disc,' or a plate that provides the pressure drop associated with a wind turbine, one can calculate the most ideal power output of the turbine. The limit for power output can be obtained assuming that there is no drag, the 'actuator disc' has no mass, all flow going into the rotor goes out of the rotor in the same direction (conservation of mass), and the flow is incompressible. It can also be assumed that any point in the fluid flow before the rotor and after the rotor is steady.

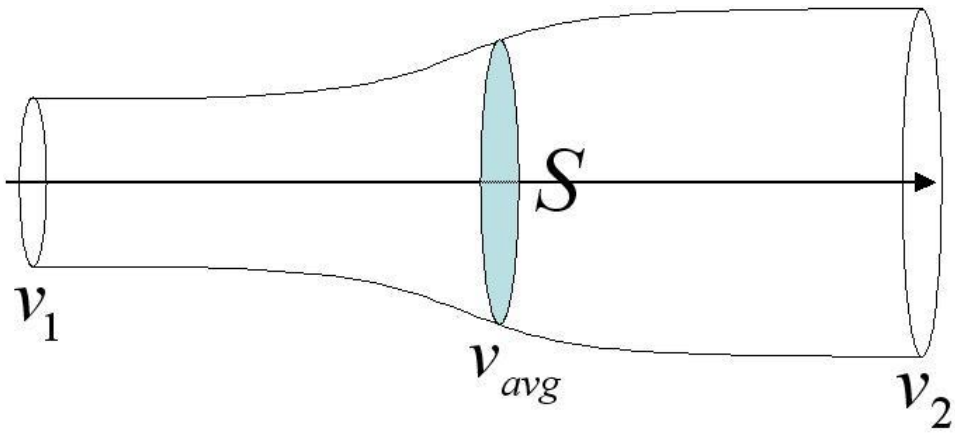

Figure 1: Flow before, during, and after the fluid has passed through the rotor.

Bernoulli's equation can be applied to a streamline from v_1 (far upstream of the turbine) to v_{avg} and from v_{avg} to v_2 (far downstream of the turbine), but not in the control volume of the actuator disc, because this is where flow is unsteady and there is a pressure drop. This pressure drop helps in calculating the power output:

$$Power = (P_1 - P_2)A_t V_{avg}$$

(1)

where A_t is the area of the rotor, P_1 is the pressure before the rotor, P_2 is the pressure after the rotor, and V_{avg} is the velocity at the rotor. From continuity, it can be assumed that

$$A_1 V_1 = A_t V_{avg} = A_2 V_2$$

(2)

The force on the fluid caused by the rotor can be calculated as:

$$F = ma = \dot{m}\Delta v = \rho A v(v_1 - v_2) = (P_1 - P_2)A_t$$

(3)

Using Bernoulli's equation solely for the fluid flow before and after the rotor,

$$P_o + \frac{1}{2}\rho v_1^2 = P_1 + \frac{1}{2}\rho v_{avg}^2$$

(4a)

$$P_o + \frac{1}{2}\rho v_2^2 = P_2 + \frac{1}{2}\rho v_{avg}^2$$

(4b)

Combining equations 2, 3, (4a), and (4b),

$$P_1 - P_2 = \frac{1}{2}\rho(v_1^2 - v_2^2) = \rho\frac{A_1}{A_t}v_1(v_1 - v_2) = \rho v_{avg}(v_1 - v_2)$$

(5)

Upon analyzing equation (5), it can be determined that velocity at the rotor is the average of the velocities before and after:

$$V_{avg} = \frac{1}{2}(V_1 + V_2)$$
(6)

And thus finally, efficiency can be given from the following equation:

$$\eta = \frac{Power}{\frac{1}{2}\rho A_t v_1^3}$$
(7)

Plotting the velocity ratios versus efficiency, the following curve can be observed:

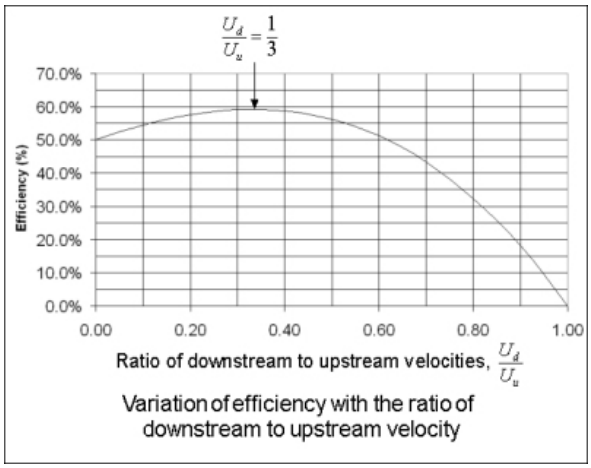

Figure 2: Plot of velocity ratios versus efficiency.

It is apparent from this plot that the highest efficiency occurs when the lowest downstream velocity is a third of the free stream velocity before the rotor. This efficiency is calculated to be 59.3%. This means that the most ideal turbine could only produce about 59% of the power that the wind exerts on it due to kinetic energy. This law is still being used today by engineers to understand the best ways to make a wind turbine the most efficient that it can be; however, there are many obstacles besides the Betz limit that prevent turbines from being more efficient, including drag, low wind speeds, and transmission losses.

Betz' Law was used in the beginning of IPRO-323 in understanding the best possible conditions for achieving the highest efficiency in building-mounted wind turbines. The surface design was influenced by this law; the airflow pattern in Figure 1 shows a curve as the air enters the rotor. This flow pattern inspired a bell-curve shape, or Gaussian shape. A shape such as this would provide The optimum acceleration for a shape such as this would occur if a turbine were placed on the back of the curve, displayed in Figure 1 as the curve going into the rotor.

Sources:
http://www.innovateus.net/earth-matters/what-betz-law
http://www.wind-power-program.com/betz.htm

http://c21.phas.ubc.ca/article/wind-turbines-betz-law-explained
http://www.math.le.ac.uk/people/ag153/homepage/Gorlov2001.pdf

Appendix F

Wind Turbine Simulation and Surface Design Prototype

Simulation of a Wind Turbine Using a Perforated Plate

Because of time and cost limitations for IPRO-323 this semester, it was obvious that creating a real turbine and calculating the actual power output of the turbine would not be viable. After reviewing the articles "Experimental study on the wind turbine wake meandering with the help of a non-rotating simplified model and of a rotating model" by S. Aubrun, S. Loyer and G. Espana from AIAA and "Wake Characteristics of two-dimensional perforated plates normal to an airstream" by Castro, it was decided that a perforated plate would suffice to imitate the wake characteristics of a turbine with a similar cross-sectional area. The mesh plate would be produced to mount to the surface design to imitate an ideal wind turbine so that the most ideal effects of the shape could be observed.

The article from AIAA tested a 3-blade wind turbine and a porous disc with the same cross sectional area to find that the wake characteristics of each were nearly identical. The idea behind this 'mock turbine' is that it acts as a drag source and creates a pressure drop across the porous plate as compared with the pressure drop across a turbine. The article helps to verify that a mesh plate with certain porosity can imitate a wind turbine, even considering the rotational effects of the turbine in the wake.

After reviewing this article, it was decided that a mesh should be used in place of a turbine. A sturdy metal plate with circular holes was cut at twelve inches in height and spanned the width of the wind tunnel. The most difficult part about using the mesh was testing its wake characteristics with a pitot tube to verify that it could be used to imitate a close-to-ideal wind turbine. This was done by testing the velocity at different distances downstream of the mesh, and using the concepts of Betz' Law to try to achieve the a third of the free stream velocity to be the lowest velocity downstream of the mesh.

Castro: The Study of Perforated Plates

After the perforated plate did not yield positive results, a review of Castro's article was done to understand the effects of different porosities of perforated plates, and the variation of velocities downstream of the mesh that was affected by the size of the mesh.Specifically, Castro researched two-dimensional perforated plates in the Reynolds number range from 25,000 to 90,000. Measurements of drag, shedding frequency, and mean velocity were made as well as turbulent intensity variation for plates of high and low porosity to study what effects these plates would have in the wake. The initial studies of Castro's work consisted of analyzing the normalized streamwise distance against the normalized downstream velocity. It can be seen that there is a

correlation between the porosity of the plate and the velocity of the flow downstream. This research was one of the influences of the previous paper that was used as a reference for replacing an actual wind turbine with a porous plate in the IPRO-323 experiment.

The main concept used from this paper was that of the varying velocities in the wake of perforated plates with different porosities. The experimentation with porosity and plate size in IPRO-323 was derived using Castro's studies, namely the following plot:

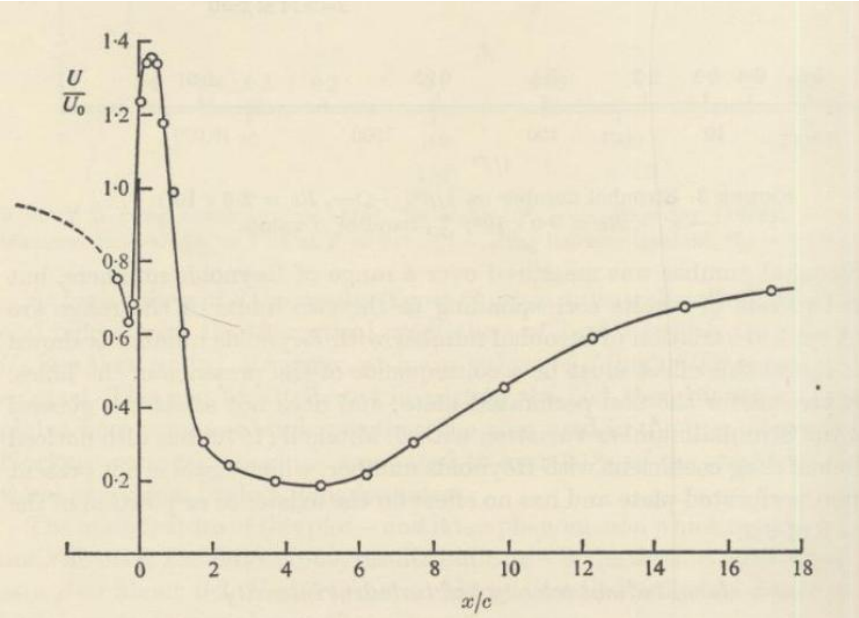

FIGURE 5. Typical variation of mean velocity behind a plate with high β. $\beta = 0{\cdot}425$ (plate 3).

Figure 3: Wake velocity variation with a porosity of 42.5% (Castro)

The goal was to find a porosity that would provide the lowest velocity of about a third of the free stream velocity so that the wake velocity would match that of an ideal wind turbine, as expressed in Betz' law in Appendix E. With Castro's data, the IPRO 323 testing team designed an experiment in which the desired downstream velocity could be found. By changing the porosity and size of the perforated plate, a minimum downstream velocity of nearly one third of the free stream velocity was observed.

The data follows the trend of the data set by Castro. The data is gathered by measuring the flow speed downstream of the mesh. Because the flow velocity ahead of the mesh is known,the flow velocity can be normalized. This V/Vo ratio is the normalized flow velocity, and is where the one-third free stream velocity is found. By shortening the chord length of the mesh we were able to get a much larger normalized chord length to downstream distance ratio, x/c. The collected data follows the same trend as the data gathered by Castro. There is a region where the turbulent effects from the mesh make taking readings difficult, and then towards the x/c mark of roughly five the flow speed is at its minimum.

In the IPRO 323 experiments the lowest normalized velocity value was within 10% of the desired value of one-third. The resulting error found was due to the mounting of the mesh. After

some experimentation and a range of error between experiments, troubleshooting found that whenever the mesh is moved or shifted in its mounting position the results would vary. To confirm this, the mesh was removed, reinserted, and tested repeatedly. It was found that when the mesh had any type of bend in its span the data would contain more error. When the mesh is mounted to the point where it was ensured that there are no anomalies, all testing data came out as expected with minimum error.

Increasing the porosity by adding a mesh sheet over the previously tested perforated plate produced surprisingly accurate results, and cutting the mesh from twelve inches to five inches helped to shorten the wake effects to a downstream length that could be measured more easily. After testing and retesting the effects of the redesigned mesh plate, it was concluded that the plate could be used to adequately imitate the flow characteristics downstream of a wind turbine by simulating the pressure change. These flow effects simulate the changes that take place downstream when energy has been extracted from the air by the turbine.

Sources:

"Experimental study on the wind turbine wake meandering with the help of a non-rotating simplified model and of a rotating model" by S. Aubrun, S. Loyer and G. Espana, Laboratoire PRISME, Universite d'Orleans, Orleans, France and P. Hayden, P. Hancock, EnFlo Laboratory, University of Surrey, Surrey, UK, American Institute of Aeronautics and Astronautics.
"Wake Characteristics of two-dimensional perforated plates normal to an airstream" by I.P. Castro, Department of Aeronautics, Imperial College, London, S.W.

Surface Design Prototype

In this IPRO the idea is to shape incoming airflow such that when it hits a turbine it will be moving faster than the free stream velocity. To accomplish this, a shape needs to be developed through research and testing. The shape that was settled on follows a basic Gaussian shape where y is in the vertical dimension, and x is in the horizontal direction. The exact specifications and a graph of the shape are shown below:

$$y = e^{(-(x^2)/2)}$$

(1)

After some research the team decided that a simple initial shape would be a good starting point to analyze the acceleration of the air flow. With help from an article out of the Journal of Aerospace Engineering it could be seen that there has been work done on airflow over specific shape types. This paper illustrates the effects that an obstacle has on the velocity of the flow near the surface. Because this data is readily available, the shape was able to be modeled after it.

The research shows that at and after the peak of the shape there is a clear increase in the flow velocity. The sizing of the shape was based upon the size of the wind tunnel. The shape needed to be able to fit into the wind tunnel while not creating a nozzle effect through the entire test section. It was decided that a height of nine inches was to be the maximum to minimize negative effects in testing.

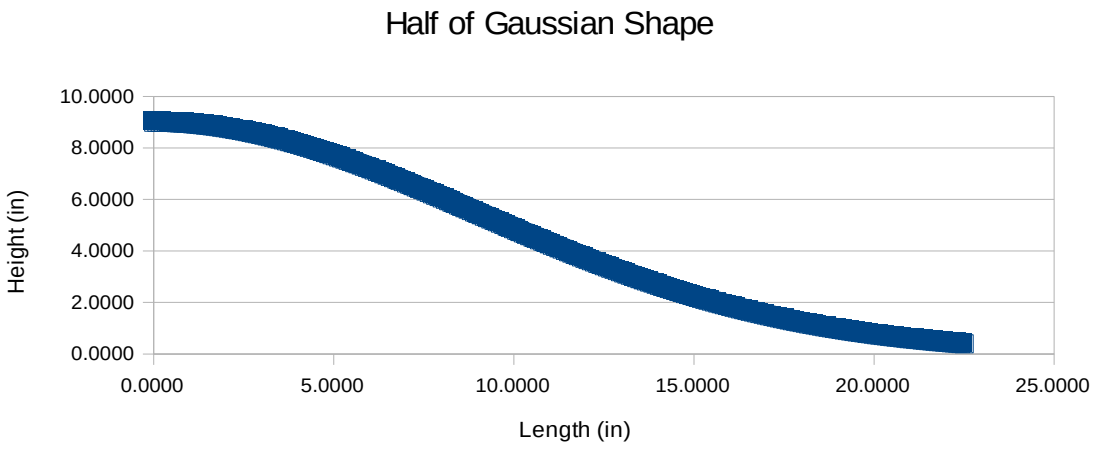

Figure 4A: A plotted version of half of the Gaussian shape used for the surface design.

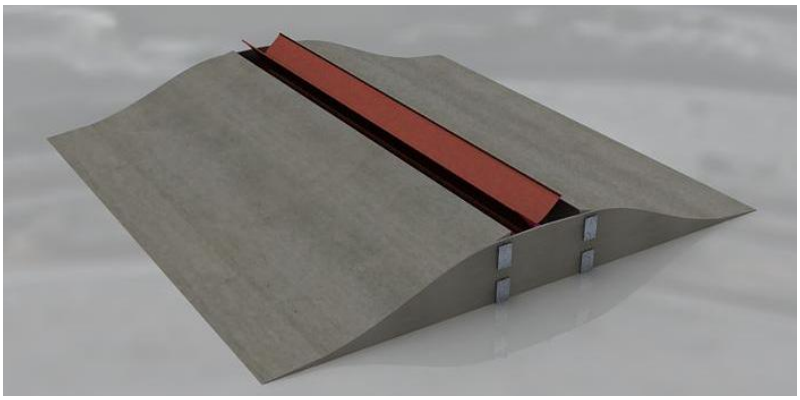

Figure 4B: An architectural rendering of the surface design with a turbine-type structure at the top.

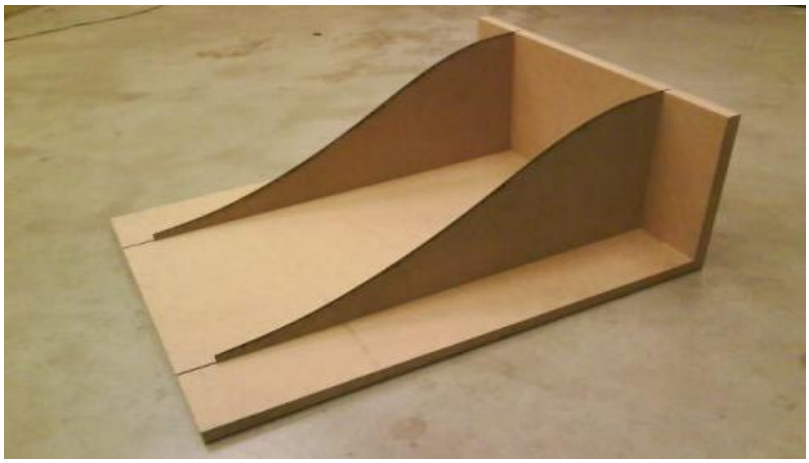

Figure 4C: A wooden guide for cutting foam into half of the Gaussian shape.

Figures 4A-4C give an idea of the shape that was decided for the first prototype, and how it was fabricated. Figure 4C shows the structure of the component used to cut a precise shape. Two half Gaussian shapes were cut and attached together to form the full shape.

Appendix G

Computational Fluid Dynamics

Computational Fluid Dynamics (CFD) is a physical-mathematical model. CFD provides a depiction of a very complicated mathematical analysis. Studying fluid flow can be done experimentally, analytically, and computationally. Each method has its advantages and disadvantages. Experimental research is invaluable because it is reality. However, conducting and experiment is often expensive and time-consuming. Analytical research has the advantage of providing insight as to why the fluid flow is behaving in the way it is. On the other hand, this

analysis is restricted to simple scenarios and geometries. It is impossible to evaluate complex fluid motion by hand. Computational research does not require the same time and money as experimental research and it is also not limited to simple scenarios and geometries. However, CFD is not reality and the computational analysis is largely based on approximations. This Interprofessional Projects uses Computational Fluid Dynamics as a means for validating the experimental research.

Computational Fluid Dynamics is a multistep process. First, the physical model (geometry) must be created, meshed, and assigned boundary conditions. Then, the mathematical model must be applied by defining the fluid and the characteristics of its motion.

Gambit is the geometry and mesh generation program used this semester. This program creates the boundaries of the wind tunnel, the perforated plate, and the flow guiding shape. The boundary conditions of the physical model must then be defined. The top and bottom of the geometry is defined as a *wall*. This represents the top and bottom of the wind tunnel. The right edge of the geometry is defined as a *velocity-inlet*. This represents the origin of the fluid motion. The left edge is defined as a *pressure-outlet*, a condition often used as an exit or escape. The perforated plate is defined as a *porous_jump*, a boundary condition that will be further defined later on in the process.

The created geometry is based upon the dimensions of the wind tunnel (68 inches tall). The CFD models used throughout this project were two-dimensional, which reflects the experimental setup. The next step is to mesh the geometry. Meshing splits the geometry into a number of control volumes, also known as cells. This is a necessary component to the computational analysis. The CFD analysis software, ***Fluent***, calculates the fluid motion at the center of each individual cell, and then combines the multiple analyses to create a flowing model. Thus, coarser mesh, with less cells, may produce a less accurate model of reality. However, creating too many cells may also produce unrealistic results because there is a possibility of over evaluating the model. For the purposes of this project, a default cell size of one unit was used. Figure 1 through 3 depicts the meshed geometries for the perforated plate, surface shape, and the perforated plate plus shape.

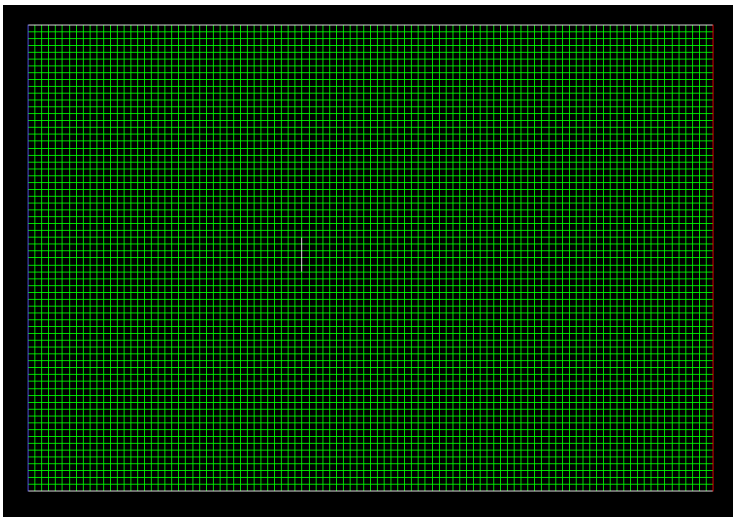

Figure 1: Meshed geometry of the perforated plate (the plate is a small white line in the left-center).

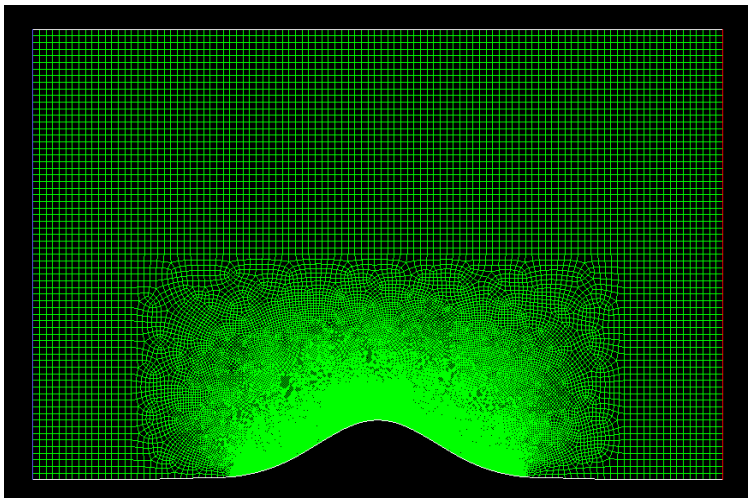

Figure 2: Meshed geometry of the flow guiding surface shape.

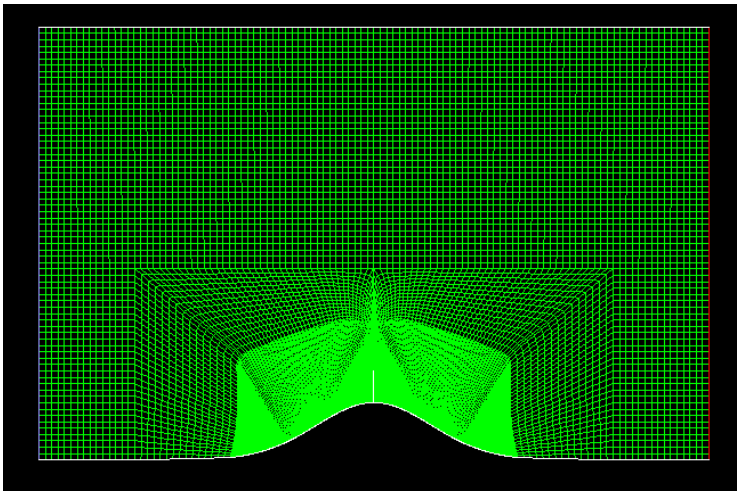

Figure 3: Meshed geometry of the plate and surface shape.

Once the geometry has been meshed and assigned boundary conditions, it must then be exported to ***Fluent***, the CFD analysis software used throughout the duration of this project. ***Fluent*** is a finite volume solver, meaning it is based upon the finite volume method for evaluating partial differential equations. The method is one of the most versatile descretization techniques used in Computational Fluid Dynamics.

Fluent allows the user to input different parameters to model the fluid flow. The first step was to model the perforated plate in the wind tunnel and ensure that the computational model accurately represents the experimental research. The *porous_jump* boundary condition was used to model the porous plate. The parameters used to define the *porous_jump* are *face permeability*, *medium thickness*, and *pressure jump coefficient*. The face permeability and pressure-jump coefficient are both a function of the fluid particle diameter and the porosity of the plate. Equations 1 and 2 define the *face permeability* and *pressure jump coefficient* for a *porous_jump* condition, respectively.

$$\alpha = \frac{D_p^2 \cdot \epsilon^3}{150(1-\epsilon)^2}$$

(1) face permeability

where α = face permeability

D_p = particle diameter

ϵ = porosity or $\frac{\text{Area of voids}}{\text{Area of plate}}$

$$C_2 = \frac{3.5\ (1-\epsilon)}{D_p \cdot \epsilon^3}$$

(2) pressure jump coefficient

where C_2 = pressure jump coefficient

The medium thickness (m) is simply the thickness of the plate. Initial values used for calculations are as follows

$D_p = 4 \times 10^{-10}$ m

$\epsilon = 0.54$

m = 0.0010795 m

Note that ***Gambit*** creates dimensionless geometries and uses a generic unit and the geometry created for this project is based on inches. ***Fluent*** uses metric dimensions, and therefore the geometry must be scaled, in ***Fluent***, to convert from inches to meters.

The *velocity-inlet* must be defined to specify the x-velocity. The initial value for the x-velocity was 2.5 m/s.

The type of model describing this simulation must also be defined. The viscous motion of the fluid is turbulent. Several turbulent models are available in ***Fluent*** and each is best suited for a specific type of flow. For this project, the k-omega standard turbulent model was selected. This model is appropriate for low-Reynolds number turbulence.

Prior to solving, initialize the simulation by, again, defining the x-velocity of the fluid. Then, choose a fair amount of iterations to run the simulation; usually over 100. Inaccurate values will be given if the number of iterations is too low. More iterations will provide a more acceptable average, and it is therefore usually more accurate. The solution may converge before completing all of the iterations, simply meaning that the calculation is over.

Fluent is helpful because it makes it possible to visualize what the fluid flow is doing. Several pictures are provided below to show specific flow characteristics.

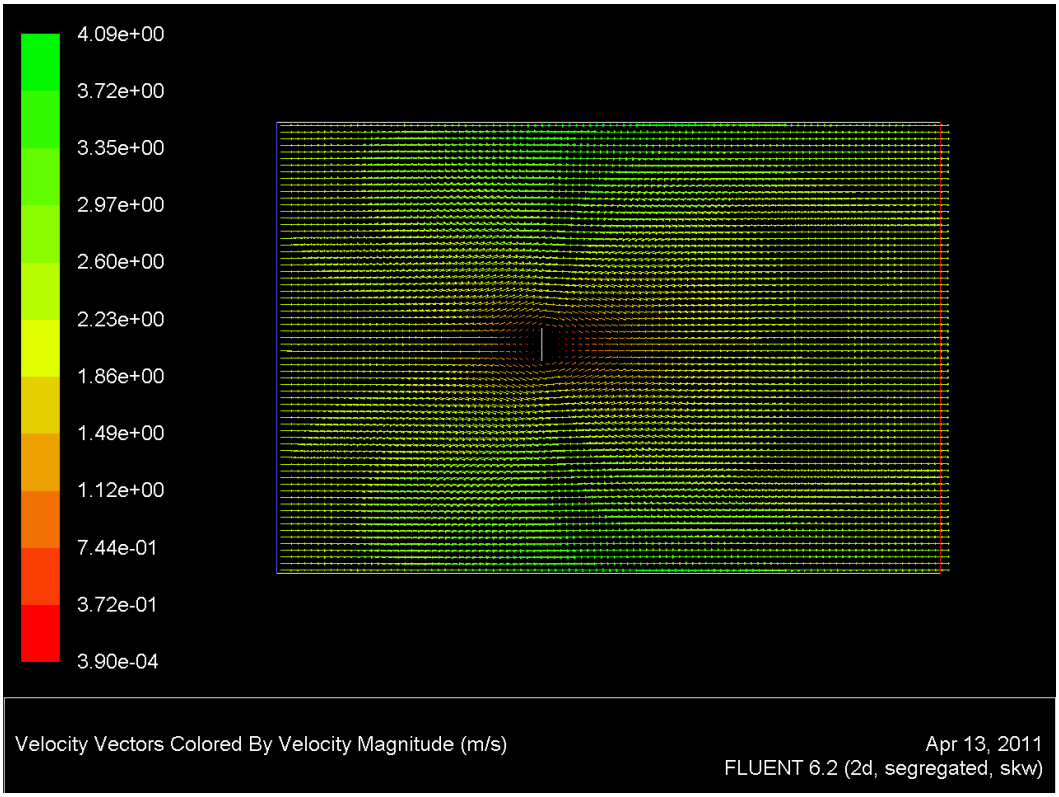

Figure 4: Velocity – perforated plate (vectors).

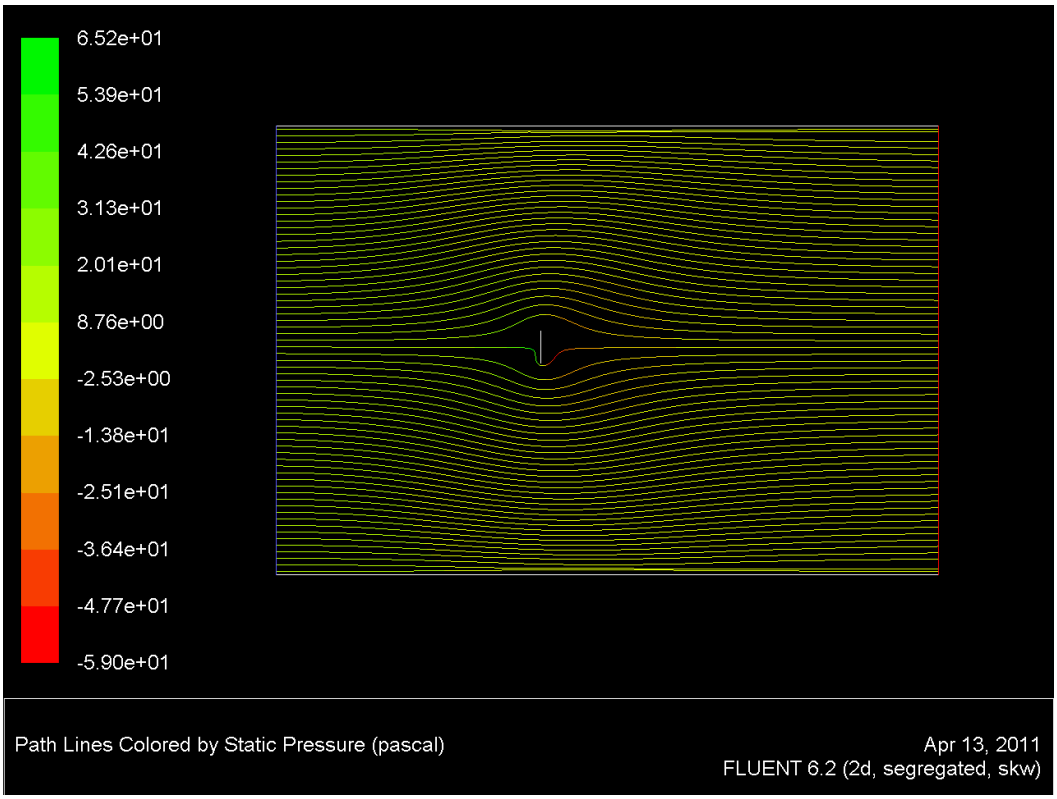

Figure 5: Static pressure-perforated plate (streamlines).

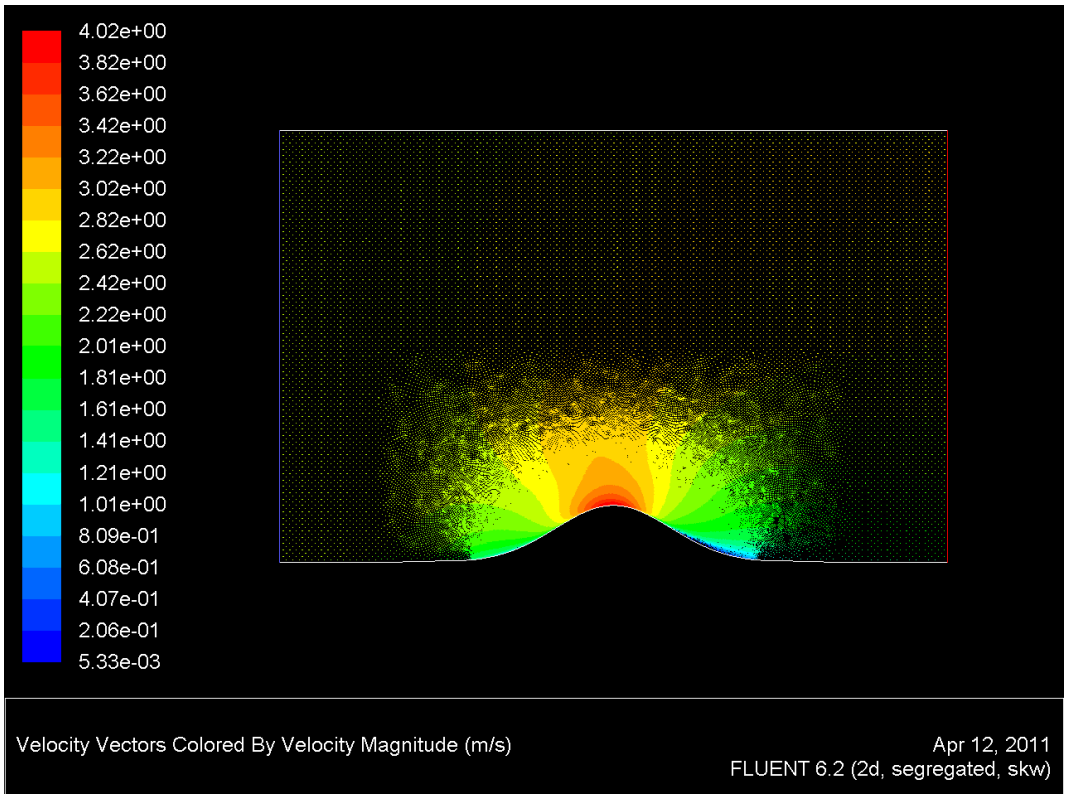

Figure 6: Velocity-surface shape (vectors).

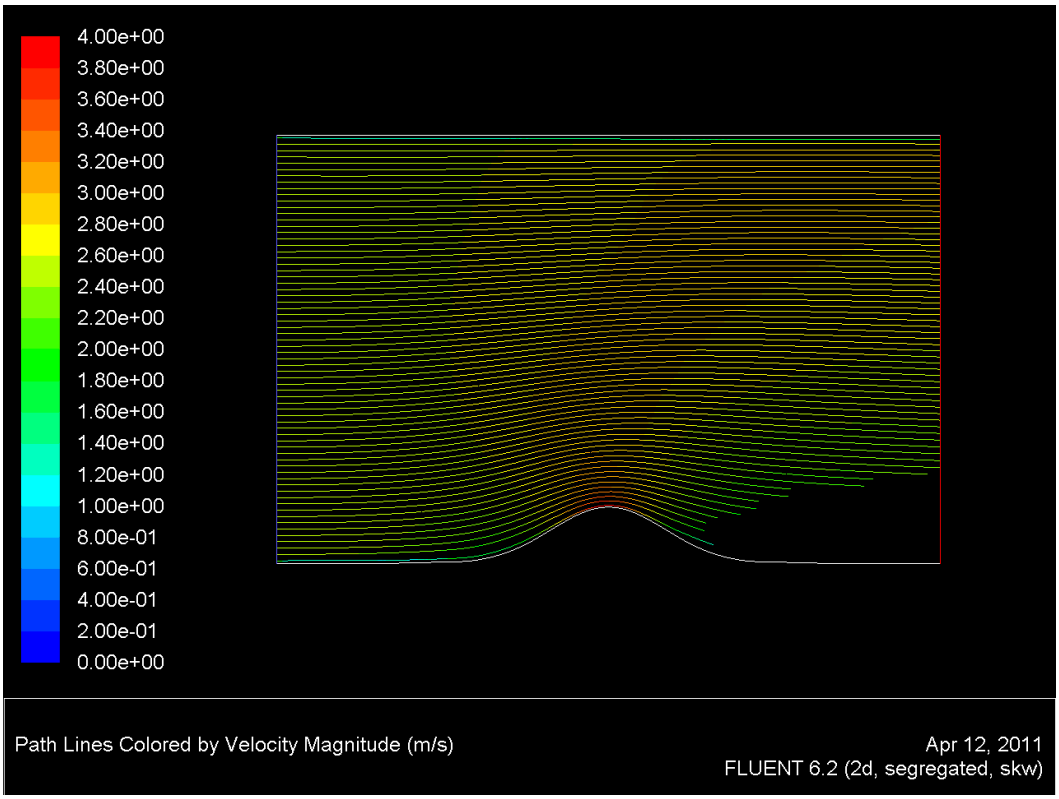

Figure 7: velocity – shape (streamlines).

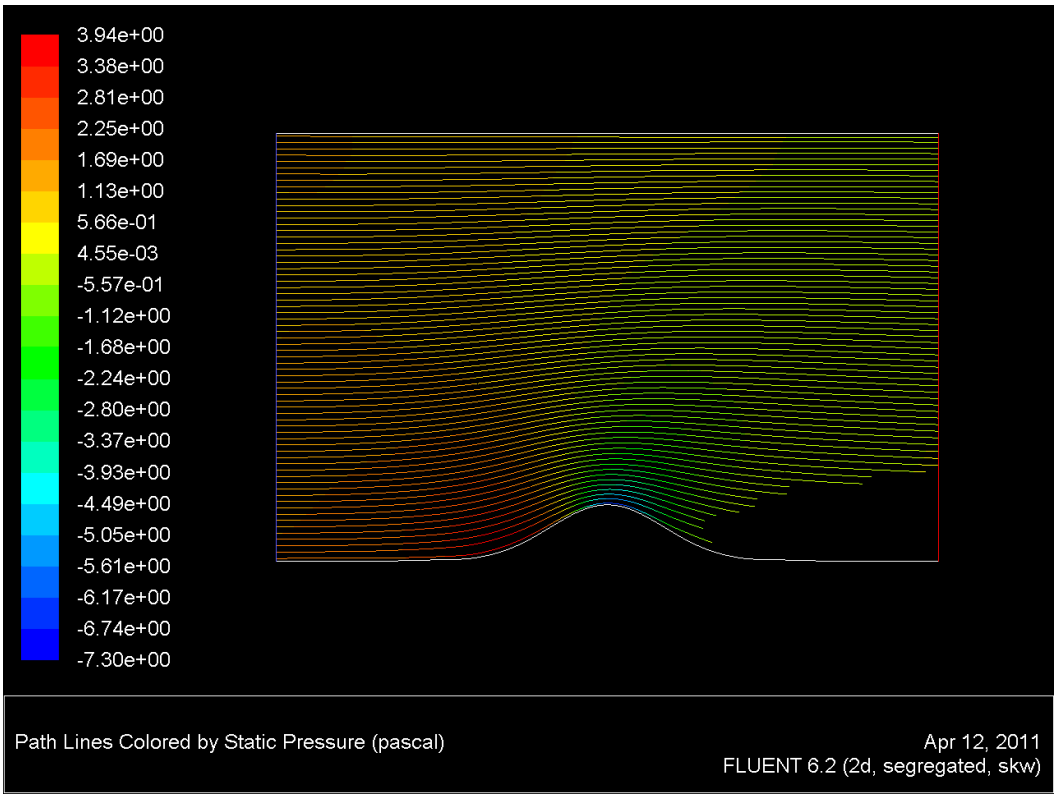

Figure 8: Static pressure-shape (streamlines).

One may find that the use of vectors or streamlines is preferable in different situations

Solving for the scenario that includes both the perforated plate and surface shape provided extremely unrealistic results. Velocities were calculated to be greater than the speed of light in some situations. Clearly, more work needs to be done. It is possible that the geometry mesh is too fine, but it is more likely that the *porous_jump* condition is no longer suitable. It is greatly suggested to change the *porous_jump* to a fan condition. This will depend on the pressure difference across the perforated plate collected from the experimental research.

PART 3: TESTING AND ANALYSIS

Appendix H

Equipment

In order to start testing in the wind tunnel, a plan was needed for what was to be measured, how it was to be measured, and what equipment and testing set-up was needed. Throughout the course of testing, it was determined that all of the following hardware was needed in order to carry out testing:

- DigiTec Temperature Sensor, Model: 5810, S/N: 65360672
- Validyne, Model: DP45-34, S/N: 43444. Demodulator, Model: CD15, S/N: 109352
- Engineering Corp Pressure Transducer, Model: DP103-10, S/N: 67548 10310N1S4D
- Keithley Autoranging Multimeter
- Pertec Peripheral Corp. Traverse System Motors, Model: PSX01 PWR.SUP, S/N: 2552
- National Instruments DAQ: 16-Input 16-bit, Model: USB 6221, S/N: E88779
- Dwyer Microtector Manometer, Model: 23-206
- M.V. Morkovin Wind Tunnel at Illinois Institute of Technology
- Pitot Tubes

Along with this hardware, a PC running the following software was also needed:

- Labview 8
- Matlab 7.4.0 (R2007a)
- Microsoft Excel

The following is a schematic of the wind tunnel dimensions and set-up for the perforated plate testing:

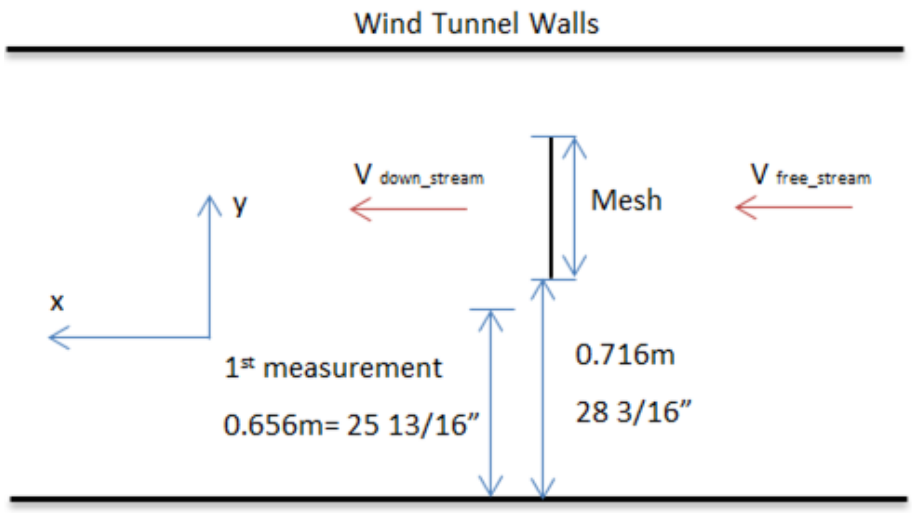

Figure 5: Diagram of the Wind Tunnel Set-Up.

Appendix I

Testing Methods, Set-Up, and Data

Pressure Transducer Calibration

After researching what was to be tested along with different testing methods, it was determined that the first step to take would be to calibrate the measurement devices, such as the pressure transducer. The transducer's main function was to take pressure measurements in the wind tunnel. The purpose of calibration was to set a standard value to begin with, and to use as the 'zero' value to understand how the transducer is affected by certain variations in velocity and pressure.The calibration of the pressure transducer provided a pressure versus transducer voltage curve, which was then linear fitted to obtain the pressure transducer coefficient (PTC). The PTC value allowed the voltage to be converted from the pressure transducer into the corresponding pressure in Pascals. The calibration was repeated multiple times to show consistency.

The manometer was used with the pressure transducer to determine the pressure versus voltage curve. The data collected is reported in the table below; figure 5 below shows the plotted data with the corresponding PTC.

W.T. Nominal	W.T. Actual (mV)	Pres. Trans. (V)	Manometer (mm)	Δh (mm)	ΔP (Pa)	Velocity (m/s)
0	0.000	-0.006	1.520	0.000	0.000	0.000
10	9.900	0.034	1.520	0.000	0.000	0.000
15	15.100	0.113	1.530	0.020	0.196	0.570
20	20.500	0.263	1.540	0.040	0.392	0.807
25	25.100	0.448	1.560	0.080	0.783	1.141

30	30.400	0.749	1.610	0.180	1.763	1.711
35	34.800	1.094	1.620	0.200	1.958	1.804
40	39.600	1.573	1.705	0.370	3.623	`
45	45.600	2.274	1.760	0.480	4.700	2.794
50	49.900	2.851	1.760	0.480	4.700	2.794
55	55.000	3.641	1.830	0.620	6.071	3.176
60	59.700	4.485	1.880	0.720	7.050	3.422
0	0.000	0.005	1.390	0.000	0.000	0.000
10	9.900	0.036	1.430	0.080	0.783	1.141
15	15.000	0.111	1.430	0.080	0.783	1.141
20	20.500	0.258	1.435	0.090	0.881	1.210
25	24.900	0.442	1.460	0.140	1.371	1.509
30	30.500	0.752	1.470	0.160	1.567	1.613
35	35.300	1.144	1.525	0.270	2.644	2.096
40	39.700	1.591	1.560	0.340	3.329	2.352
45	44.800	2.144	1.595	0.410	4.015	2.582
50	49.300	2.758	1.670	0.560	5.484	3.018
55	55.000	3.608	1.715	0.650	6.365	3.252
60	59.900	4.494	1.810	0.840	8.226	3.696
0	0.000	0.001	1.405	0.030	0.294	0.699
0	0.000	0.005	1.610	0.000	0.000	0.000
10	10.000	0.036	1.625	0.030	0.294	0.699
15	15.100	0.114	1.630	0.040	0.392	0.807
20	19.900	0.234	1.650	0.080	0.783	1.141
25	24.900	0.421	1.660	0.100	0.979	1.275
30	30.200	0.711	1.705	0.190	1.861	1.758
35	35.000	1.069	1.730	0.240	2.350	1.976
40	40.100	1.566	1.770	0.320	3.134	2.281
45	45.100	2.115	1.870	0.520	5.092	2.908
50	50.100	2.777	1.880	0.540	5.288	2.964
55	55.000	3.517	1.950	0.680	6.659	3.326
60	59.900	4.351	1.995	0.770	7.540	3.539
65	65.100	5.358	2.060	0.900	8.813	3.826
0	0.000	0.007	1.660	0.100	0.979	1.275

Table 1: PTC data collection

Note:

- Δh is double the difference in height between the manometer height at corresponding voltage setting and the zero offset.
- $\Delta P = \Delta h \rho_{H20} g$ where Δh is in meters, g=9.81 m/s^2, and ρ_{H2O}=998.2 kg/m^3
- $Velocity = \sqrt{\frac{2\Delta P}{\rho_{air}}}$, where ρ_{air}=1.204 kg/m^3

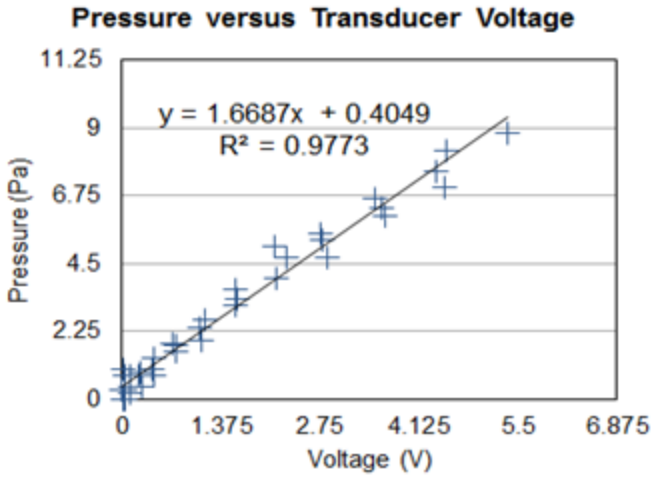

Figure 6: Calibration data from 02.03.11

The pressure transducer coefficient used to convert voltage to pressure was determined to be 1.6687 Pa/V.

Perforated Plate Testing

The first testing was done on a perforated plate to verify that it simulated the wake effects of an ideal turbine. Because this is a very hard thing to do, changes were made to the perforated plate throughout its testing in order to more closely match the wake effects of an ideal wind turbine. These changes were based on the paper referenced in Appendix F, which studied the wake effects of perforated plates with varying porosities and sizes (Castro). Because of the nature of Castro's research, it was determined that velocity measurements would be made downstream of the plate to observe the effects the plate had on the airflow after passing through it.

Verification of Spanwise Uniformity Behind Perforated Plate

As a first step to understanding the optimization of wind turbines, IPRO-323 team decided to perform a 2-D analysis. To this end, the perforated plate that simulates the same pressure drop as that shown by a generic wind turbine needs to represent a two dimensional analysis, in other words, simulate an infinitely long turbine in the axis perpendicular to both the free stream velocity and the perforated plate height (or chord). To verify that the 2-D analysis is a realistic approximation of the IPRO's experimental set-up, a spanwise uniformity was be tested. To this end, velocity measurements were taken in the flow direction and vertical direction (parallel to the perforated plate height) at three different spanwise locations. The data acquired did not change significantly with the change of the spanwise location, this verifies the 2-D assumption is realistic for our experimental set-up and 2-D fluid equations apply.

Power from Perforated Plate

Because the perforated plate was built to simulate the best wind turbine efficiency physically possible (Betz' limit), the power obtained from the perforated plate without the flow guiding structure is found with the following equation 1, using a C_p = 0.593.

$$P = 0.5\rho S U_\infty^3 C_p \quad \textbf{(1)}$$

Here, P is the power output, ρ is the air density, S is the area of the perforated plate (simulating the area of the wind turbine perpendicular to the flow and exposed to the free-stream), U_∞ is the free-stream velocity and C_p is the power coefficient. For non-ideal or real wind turbines, Cp is less than 0.593 (or 59.3% efficiency). Therefore, to obtain the power output of the wind turbine representation standing on the flow guiding structure, the following equation 2 was used and the efficiency factor or power coefficient was calculated using equation 3.

$$P = \Delta p S U_\infty \quad \textbf{(2)}$$

$$Cp = \frac{P}{0.5\rho S U_\infty^3} \quad \textbf{(3)}$$

The pressure difference, Δp, was measured with a couple of pitot-tubes; one at front and another at the back of the perforated plate, both at 4.25 inches away from the plate.

LabView Virtual Instrument Screenshots and Explanations

National Instruments LabView is graphic programming software that allows translating physical measurements into computer files. This programming tool is also called a "virtual instrument" because while the physical instruments (i.e. pitot-tube, pressure transducer, etc.) translate a physical phenomenon into a voltage that is later translated into a digital signal by the use of the DAQX, the VI (virtual instrument) takes the signal and allows the user to manage, visualize and store data. The "front panel" which is the interfaces where input conditions are set (where and how data will be collected, as well as where is the data going to be stored and where the calibration files are located), the result can also be visualized on this window.

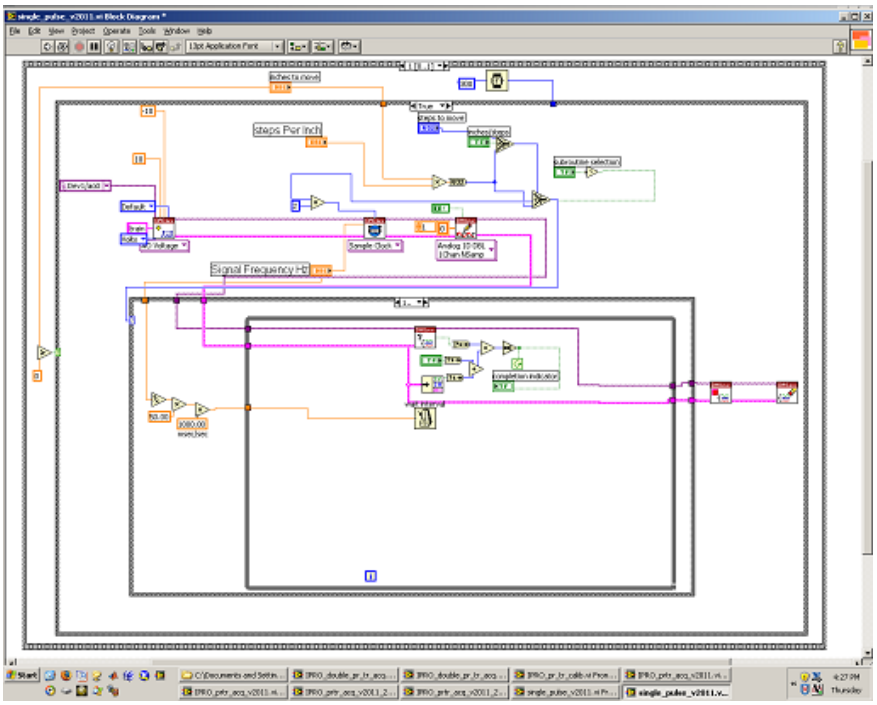

Figure 7: LabView block diagram for the motor of the traverse.

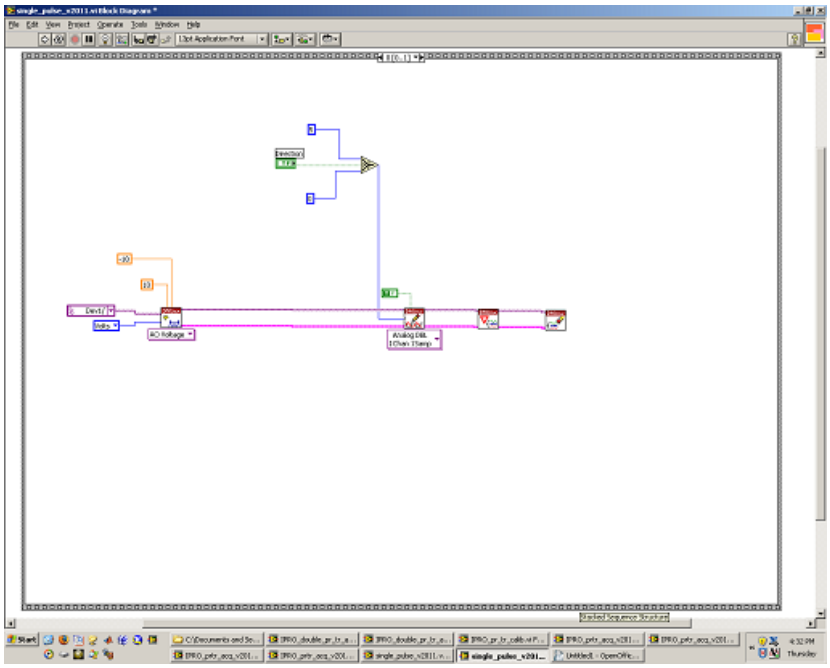

Figure 8: LabView block diagram for the motor of the traverse (Continued).

Figures 7 and 8 show “block diagrams” which are the interfaces that allow the user to manage, store data, and apply calibration factors among other things. One of these block diagrams also allows the user to set the vertical locations were data is to be taken; this allowed the team to take data automatically at different vertical locations by controlling a motor with the VI.

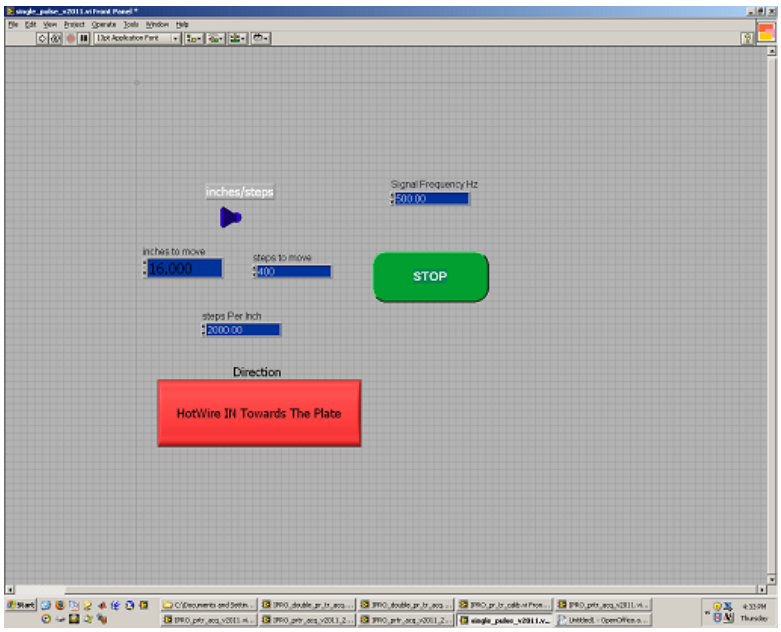

Figure 9: LabView VI for the motor of the traverse system.

This VI controlled the motor of the traverse so that the pitot tube could be lifted or lowered a certain amount of inches in the vertical direction.

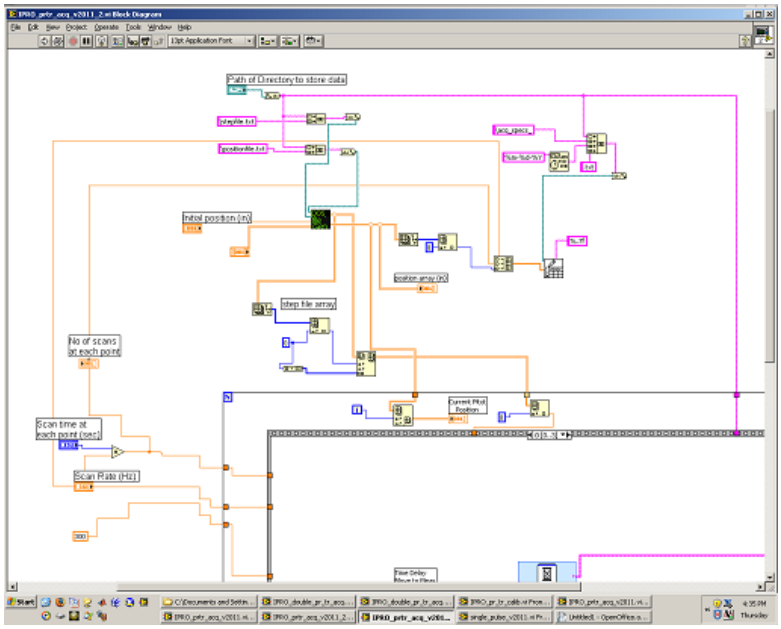

Figure 10: LabView block diagram for pressure measurements.

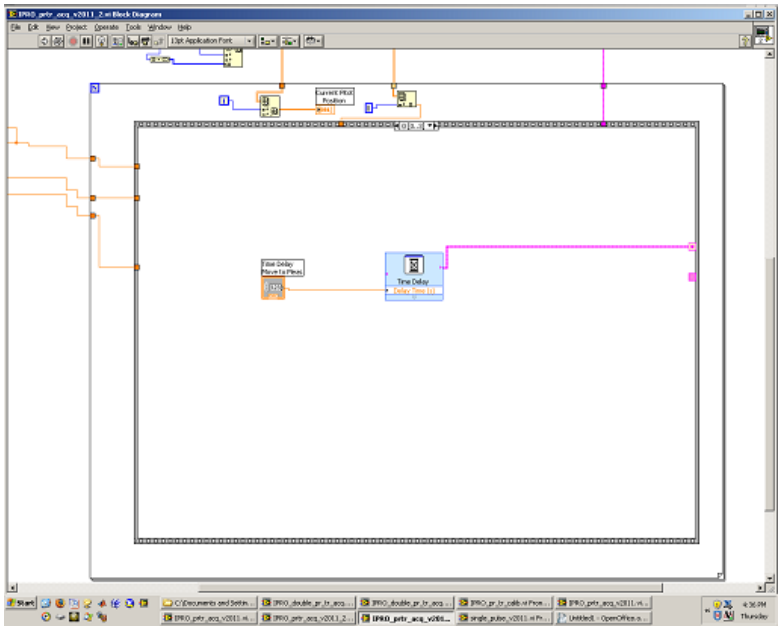

Figure 11: LabView block diagram for pressure measurements (Continued).

The "front panel" is the interface where input conditions are set. Figure 9 above shows the front panel of the motor control VI; however there were also front panels for the VIs for pressure transducer and velocity measurements:

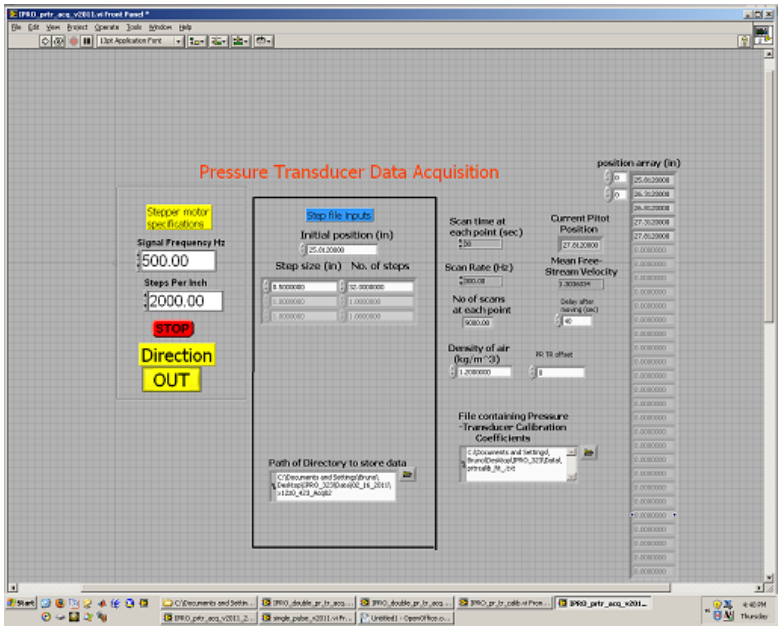

Figure 12: LabView VI front panel for pressure transducer measurements and traverse control.

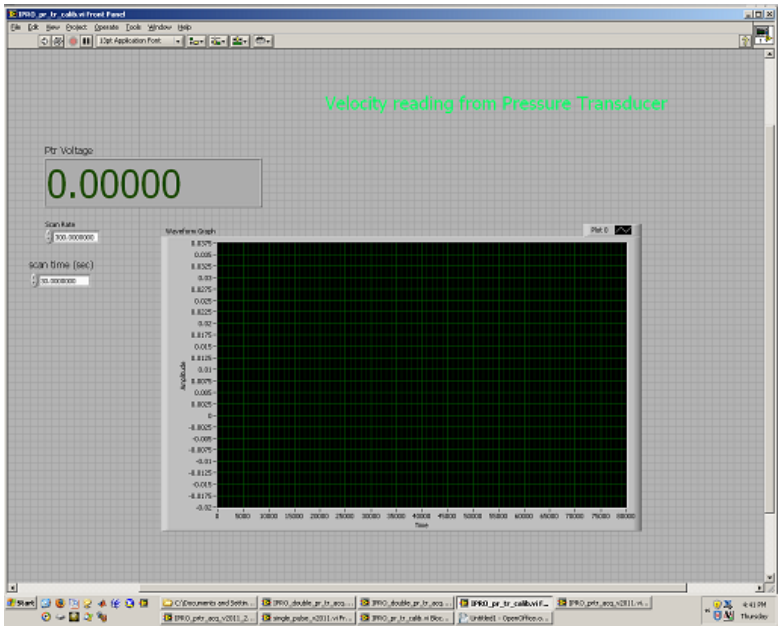

Figure 13: LabView VI front panel for velocity measurements in the wind tunnel.

The block diagram for a simple VI such as the one in Figure 13 looks like this:

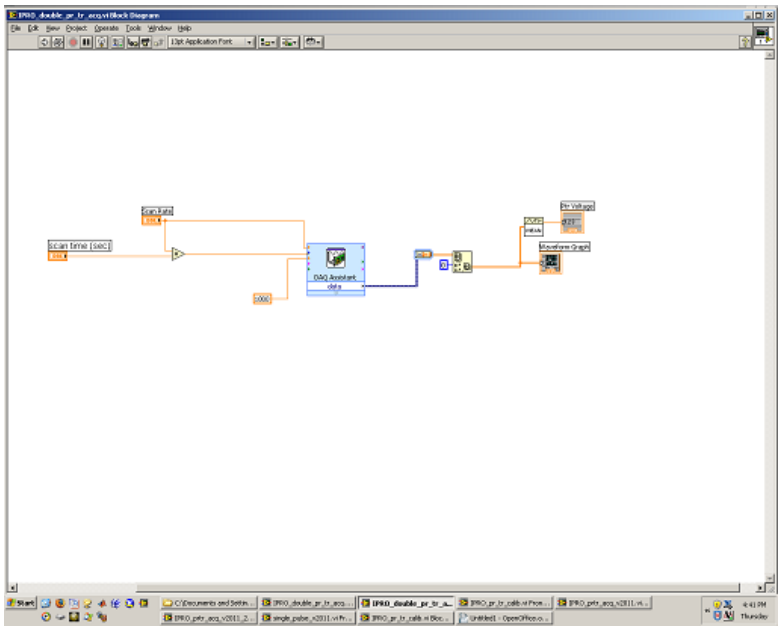

Figure 14: LabView block diagram for velocity measurements.

As you can see, the block diagram's most necessary component is the DAQ assistant, or data acquisition assistant. These VIs were necessary to control the traverse motor to make the pitot tube move, to take pressure measurements while at different vertical locations, and to simply take velocity measurements. They were essential for the testing method described in the next section.

Testing Method and Analysis of Perforated Plate Measurements

The method used to collect velocity measurements with the perforated plate involved first hooking up a pitot tube to a moveable mount located in the wind tunnel. The moveable mount allows for the pitot tube to be translated both up and down (y-direction) and in the free stream direction (x-direction). The wind tunnel was set to a constant power and thus constant free stream velocity. The pitot tube was then positioned at various x locations and varied along the y direction using the Labview VI as described in the section above. Data was obtained at x-locations downstream of the mesh so as to determine the flow speed reduction behind the mesh relative to the free stream velocity. The free stream velocity in front of the plate was taken to be 2.5 m/s as the wind tunnel conditions at that operating power were known a priori. The pitot tube was hooked up to a pressure transducer and the output from the pressure transducer was a voltage. That voltage was then converted to a pressure value using the pressure voltage calibration curve. That pressure value is in fact a pressure difference between the dynamic and static pressure. Using that pressure difference, the density of air (1.225 kg/m^2), and Bernoulli's equation the stream wise velocity was then determined. The velocity data and y-location data was recorded using the Labview VI and the x-location was determined and recorded by hand.

The following are from testing the velocity at vertical distances above, in the middle, and below the plate at distances of 3, 6, 9, 12, 15, 18, and 21 inches downstream of it:

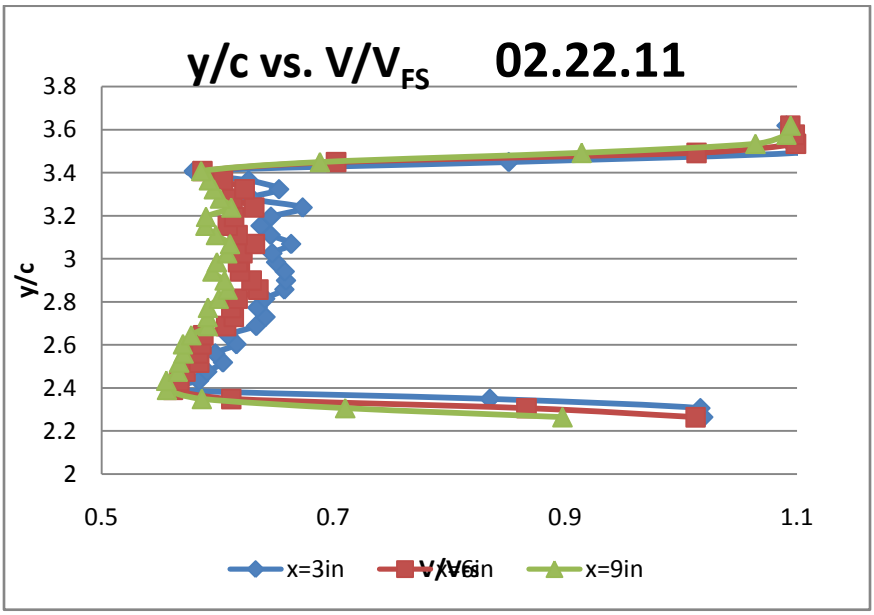

Figure 15: Vertical velocities 3, 6, and 9 inches downstream of the mesh.

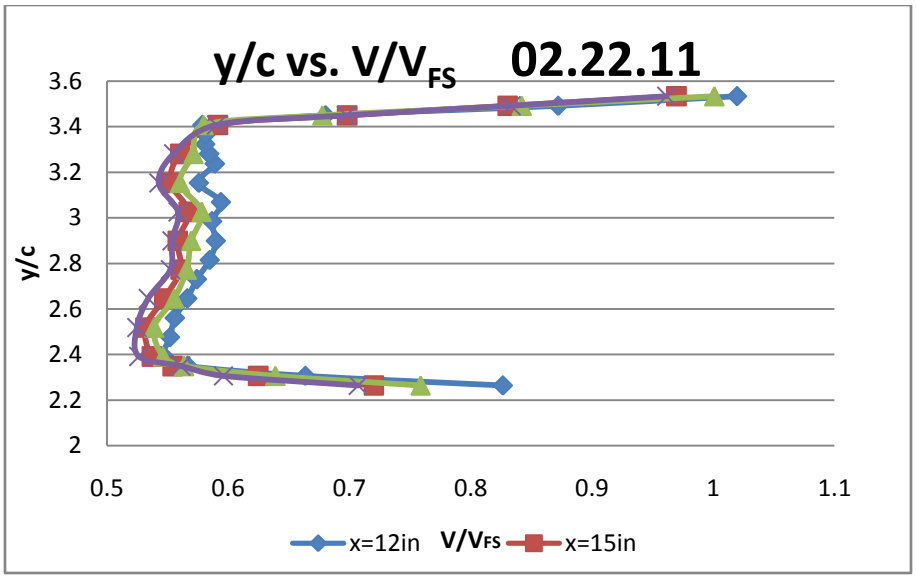

Figure 16: Vertical velocities 12, 15, 18 and 21 inches downstream of the mesh.

These curves show a normalized position versus velocity plot. It should be noted that the lowest velocity downstream of the plate only goes down to about 52% of the free stream velocity. This value is nowhere near the one-third value determined to be needed to simulate an ideal turbine.

After doing more research, a new perforated plate with a different porosity and size was made. The porosity was decreased by adding a new mesh atop the original plate. Porosity was measured by taking a square inch of the perforated plate and counting the number and size of the holes in the plate. The plate was also cut from twelve to five inches vertically so that the wake effects would not have to be measured at such far distances downstream. These changes were made in reference to Castro's studies described in Appendix F.

Figure 16B: The modified perforated plate five inches in height.

The pressure drop was also measured with a pitot tube in front of and behind the perforated plate. These results would be plotted with the pressure drop data for both the shape and the plate to compare the power outputs of the plate with and without the shape. The testing set-up to measure this pressure drop across the plate looked like this:

Figure 16C: Testing set-up to measure the change in pressure and velocity across the plate.

The data from the set-up in Figure 16C would be used later to compare to the results of the same set-up with the surface design added.

The following are plots of the vertical displacement versus velocity for the refined perforated plate:

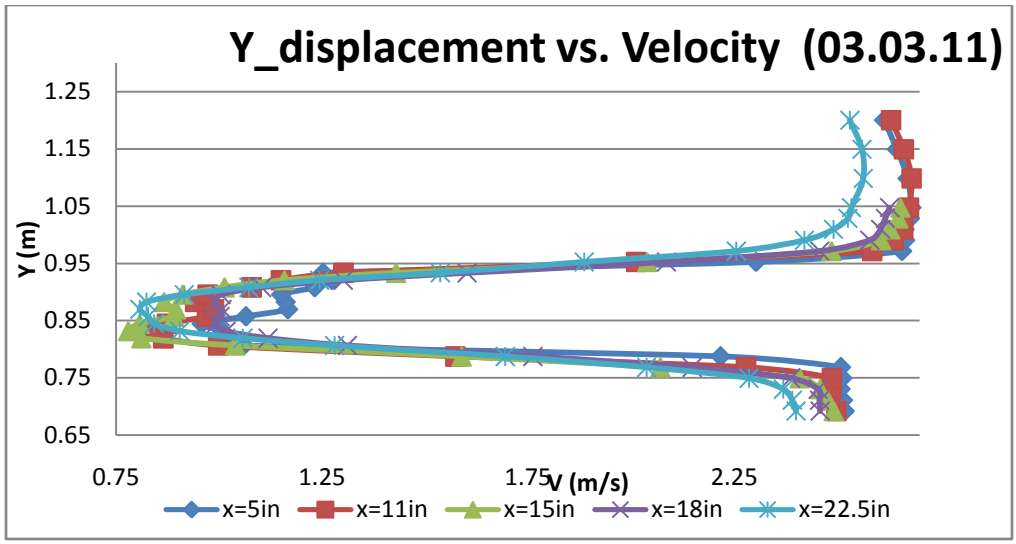

Figure 17: Y-Displacement vs. Velocity at 5, 11, 15, 18, and 22.5 inches downstream.

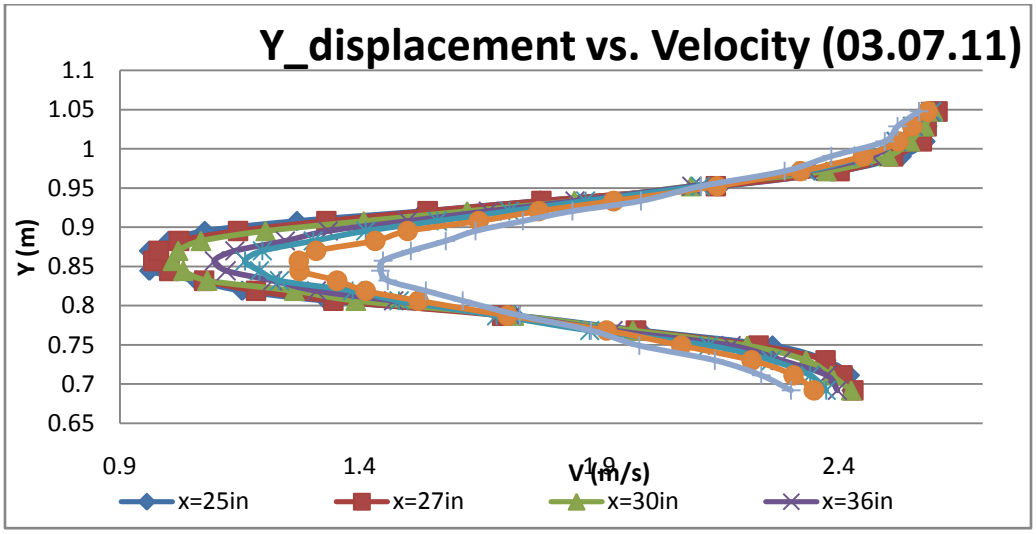

Figure 18: Y-Displacement vs. Velocity at 25, 27, 30 and 36 inches downstream.

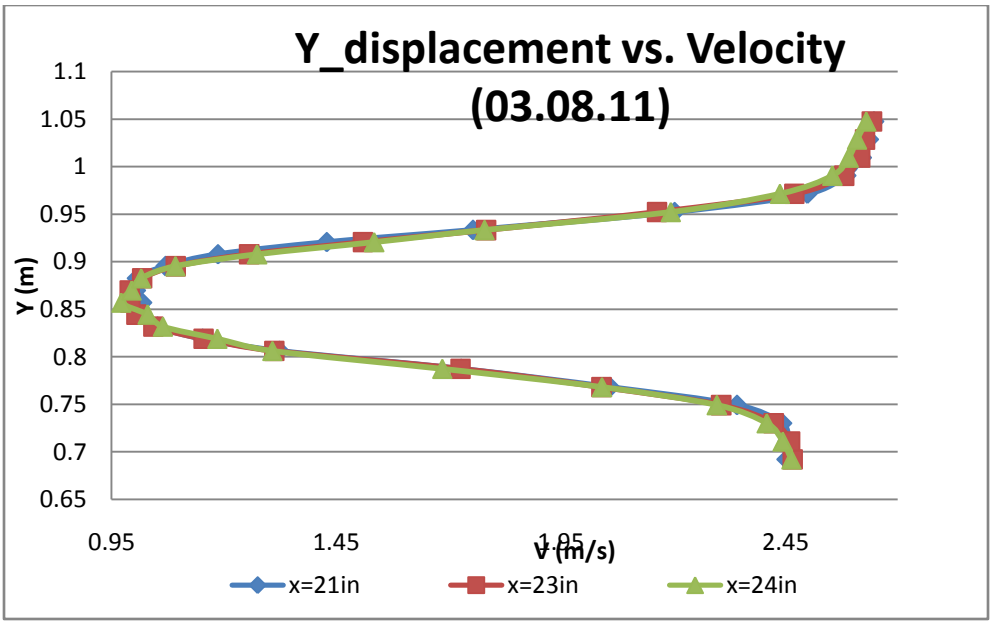

Figure 19: Y-Displacement vs. Velocity at 21, 23, and 24 inches downstream.

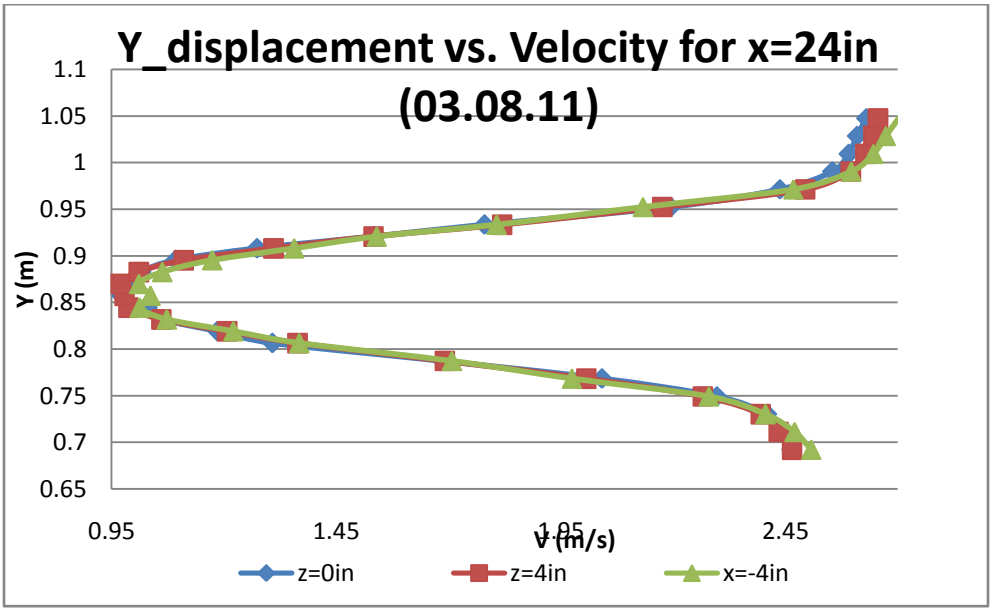

Figure 20: Y-Displacement vs. Velocity at 24 inches downstream in different positions parallel to the plate.

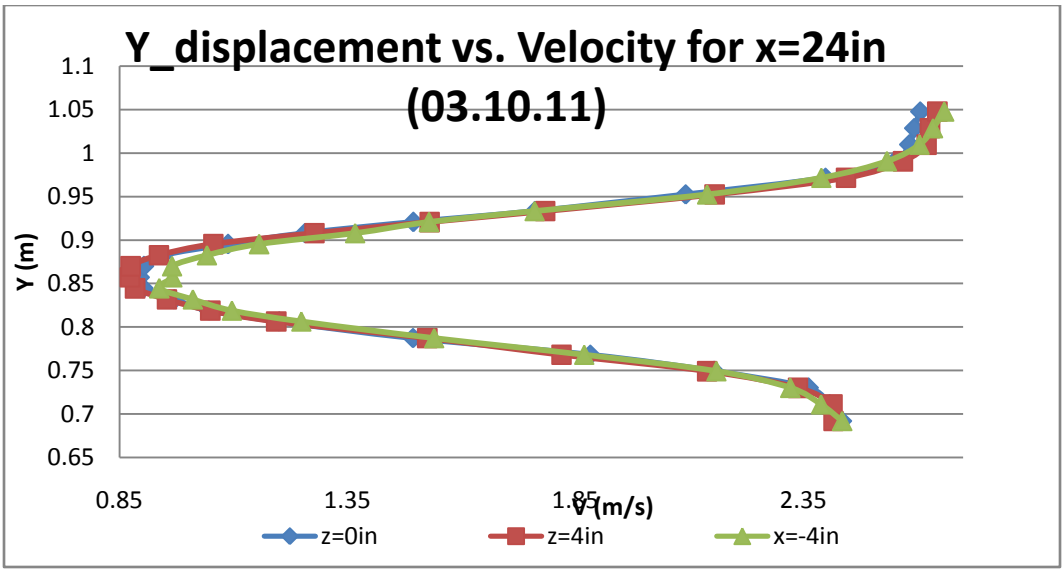

Figure 21: Y-Displacement vs. Velocity at 24 inches downstream in different positions parallel to the plate, tested for repeatability.

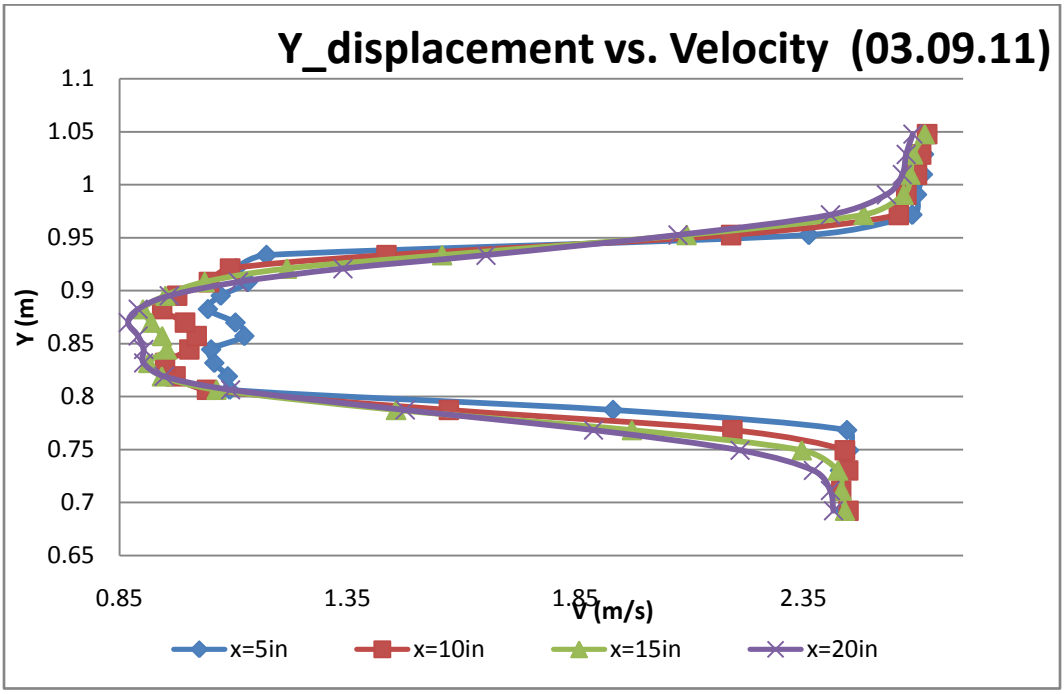

Figure 22: Y-Displacement vs. Velocity at 5, 10, 15, and 20 inches downstream.

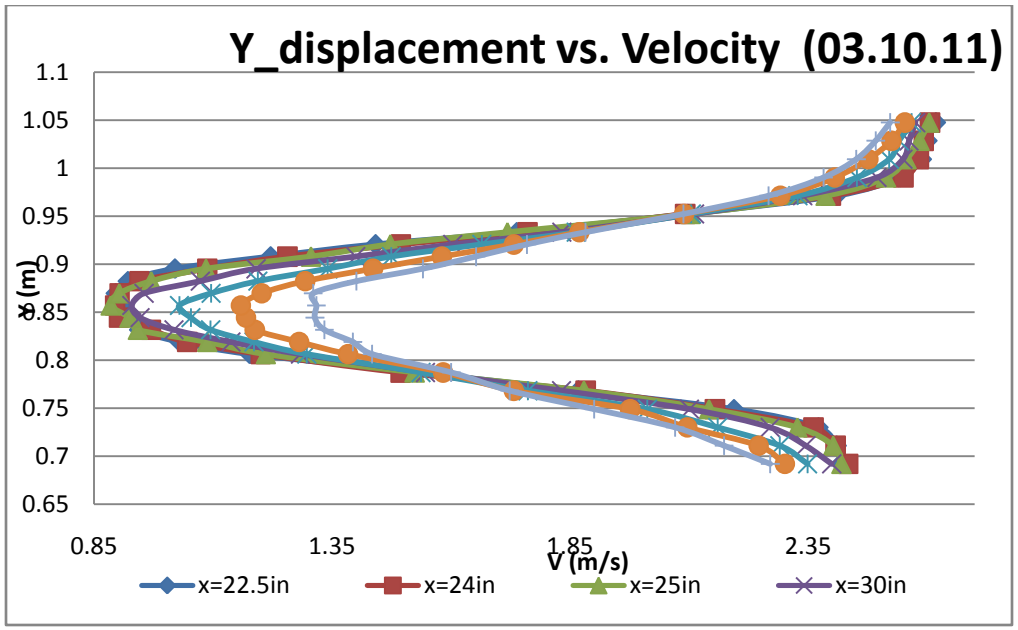

Figure 23: Y-Displacement vs. Velocity at 22.5, 24, 25, and 30 inches downstream.

The above plots show the repeatability of the results for the new mesh. The next series of graphs will show something very interesting by plotting the ratio of the y-displacement to centerline versus the ratio of velocity to free stream velocity:

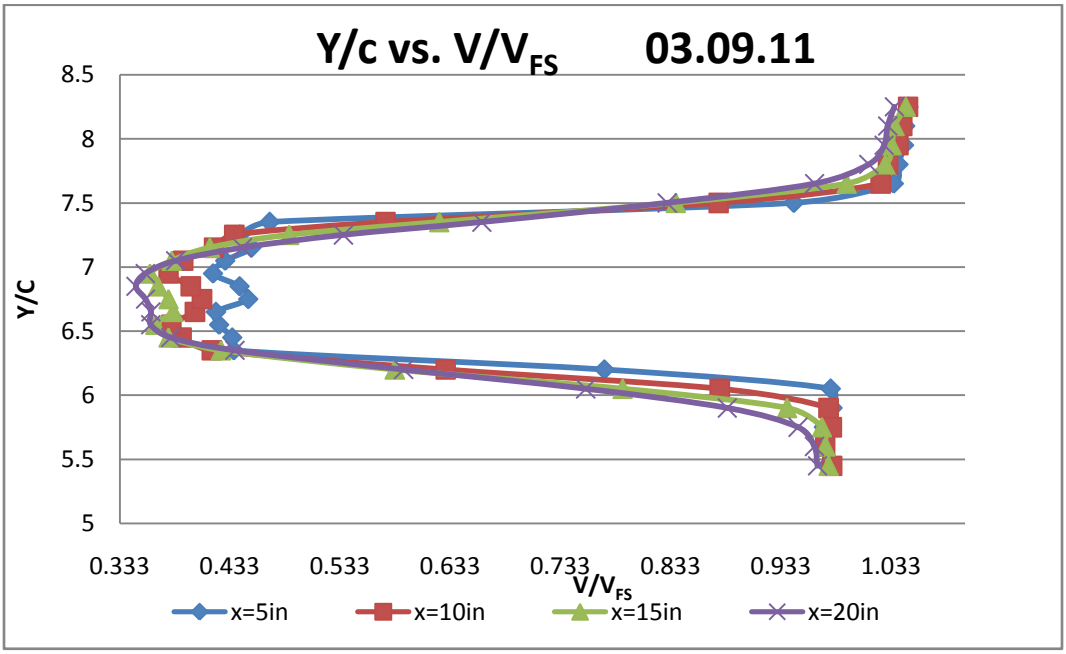

Figure 24: Normalized Y-Displacement vs. Velocity at 5, 10, 15, and 20 inches downstream.

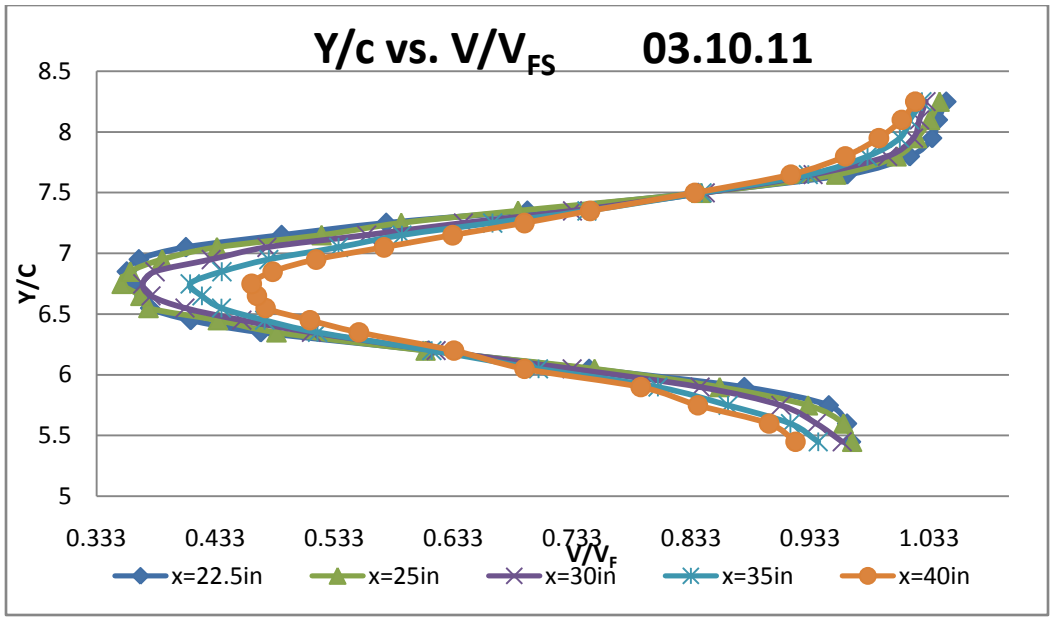

Figure 25: Normalized Y-Displacement vs. Velocity at 22.5, 25, 30, 35, and 40 inches downstream.

The following graph shows another result of the velocity ratio versus streamwise distance downstream of the mesh to verify a correlation between the IPRO 323 experiment and Castro's various experiments with porosity in perforated plates:

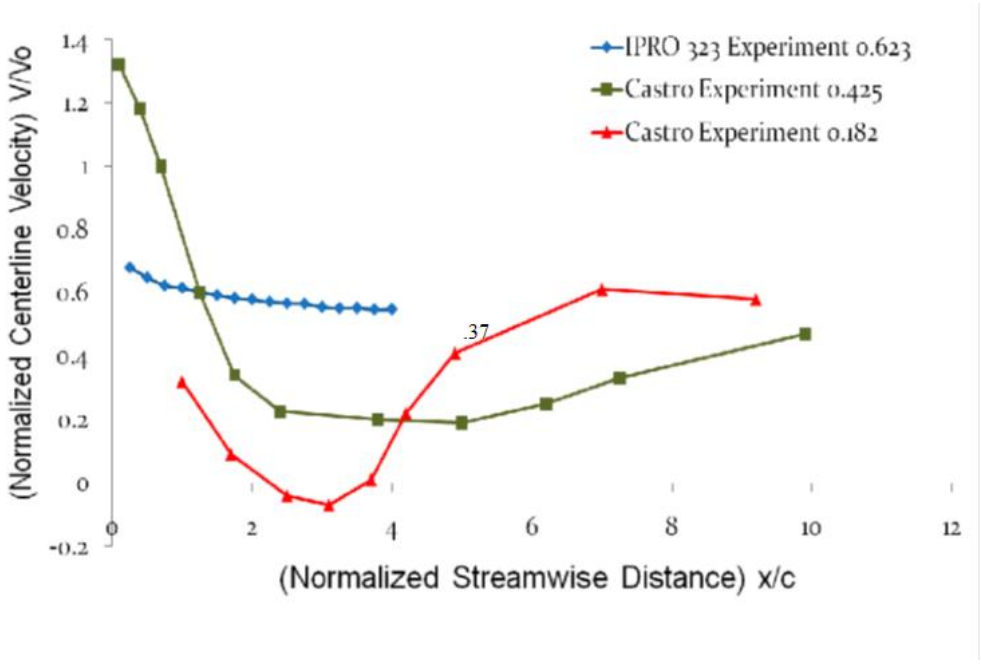

Figure 26A: Normalized centerline velocity vs. streamwise distance to verify Castro's porosity experiments.

It can be observed from Figure 13 that the IPRO 313 experiment with a porosity of 62.3% did not seem to correlate with Castro's data, and the amount of data that could be taken for the wake effects was limited by the size of the wind tunnel. As explained in Appendix F, the size of the mesh had to be altered so that more effects could be seen in the span in the x-direction. The mesh used in Figure 26A was twelve inches in height, so its effects spanned farther downstream than could be measured in the wind tunnel. After the mesh was cut down to five inches and the porosity was decreased, better results were observed:

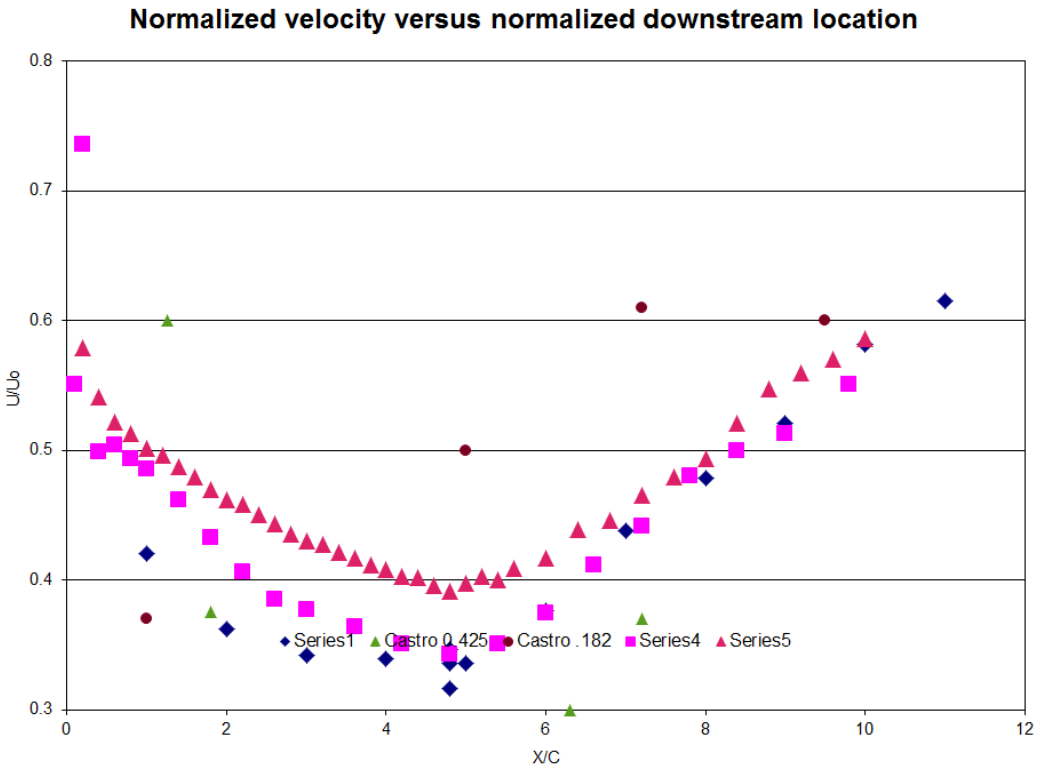

Figure 26B*: *Velocity ratio versus normalized downstream locationof the wake of the modified mesh.

Notice that the lowest velocity approaches approximately one third of the free stream velocity! These results as well as the velocity results testing in the y-direction showed that the new mesh could indeed be used to simulate the wake effects and pressure drop of an ideal wind turbine. The next step in testing could begin after this was verified.

SurfaceDesignTesting

The next step in the experiment was to gather data regarding the velocity change over the surface of the shape to verify an increase in energy at the maximum height and immediately after it.The shape was manufactured using pink insulating foam. Once completed, a testing methodology was developed where the air velocity over the shape at different x-locations was recorded. The first

set of data consisted of recording the flow velocity at a constant distance of 2.5 inches away from the shape. The x-location of the shape ranged from the front of shape (+22.5 inches) to the back of the shape (-22.5inches). The tallest point of the shape is 9 inches in height from the wind tunnel floor, and it is the origin of the coordinate system (x = 0 inches). The first set of data is reported in the table below.

Upstream			
x (in)	y (in)	Voltage (V)	V (m/s)
0	11.5	2.70402	2.841
2.5	11.159	2.61731	2.794
7.5	8.859	1.53942	2.133
12.5	5.93	0.65255	1.365
17.5	3.859	0.43506	1.098
22.5	2.895	0.44703	1.115
Downstream			
x (in)	y (in)	Voltage (V)	V (m/s)
0	11.5	2.70151	2.84
-2.5	11.159	2.68322	2.83
-7.5	8.859	1.84326	2.338
-12.5	5.93	0.25387	0.811
-17.5	3.859	0.06324	0.285
-22.5	2.895	0.12766	0.526

Table 2: Data for the velocity over the shape

Note that upstream means moving against the flow direction. The x-location vs. velocity was then plotted to understand the flow behavior over the shape, and to identify the point with the highest velocity. The plot is shown below.

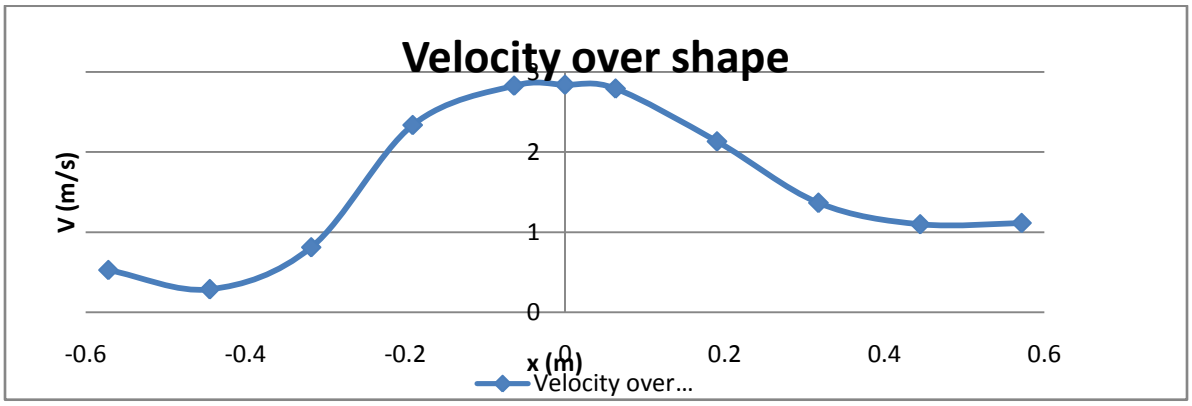

Figure 27: Velocity over the shape at different x-locations

The next set of data involved taking velocity measurements at the center line of the shape (at x=0inches) and varying the y distance from the peak of the curve. The data recorded is reported in the following table.

y (in)	Voltage (V)	V (m/s)
0.125	2.33511	2.637
0.25	2.78827	2.886
0.375	2.9806	2.985
0.5	3.10219	3.046
0.75	2.9403	2.964
1	2.91662	2.952
1.5	2.88867	2.938
2	2.76046	2.871
2.5	2.57849	2.773

Table 3: Velocity from centerline at different y locations.

It can be concluded from the velocity data testing solely the shape that the velocity nearly doubles at the maximum height. After verifying these results, the next step was to test the shape with the perforated plate on top of it to simulate a wind turbine mounted onto the surface.

Surface Design and Perforated Plate Testing

A new testing set-up was required for testing the surface design and the perforated plate together. The traverse was useless in this experiment because the main purpose in testing both components together was to find the pressure drop and velocity difference to calculate the power output of the simulated wind turbine.

The methods used to collect data with the flow guiding structure and the mesh involved using two twin pitot tubes, a pressure transducer, and a U-tube manometer. The two pitot tubes were positioned on both sides of the mesh offset from each other in the span wise (z) direction so as to mitigate any interference from the upstream pitot tube on the downstream pitot tube. The positions of the pitot tube remained constant as they were fixed relative to the flow guiding structure. The two pitot tubes were hooked up to the manometer which output the pressure difference between the upstream and downstream pitot tubes. The wind tunnel flow speed was varied by varying the wind tunnel voltage (and thus the wind tunnel power). In addition to being hooked up to the downstream pitot tube, the upstream pitot tube was hooked up to a static port and a pressure transducer in order to determine the wind speed at the different wind tunnel voltages. The values manually recorded included the wind tunnel voltage, the manometer pressure difference reading, and the pressure transducer voltage which could later be converted to a velocity reading as outlined in the section describing the methodology of obtaining velocity data with just the mesh.

The testing set-up in the wind tunnel looked as follows:

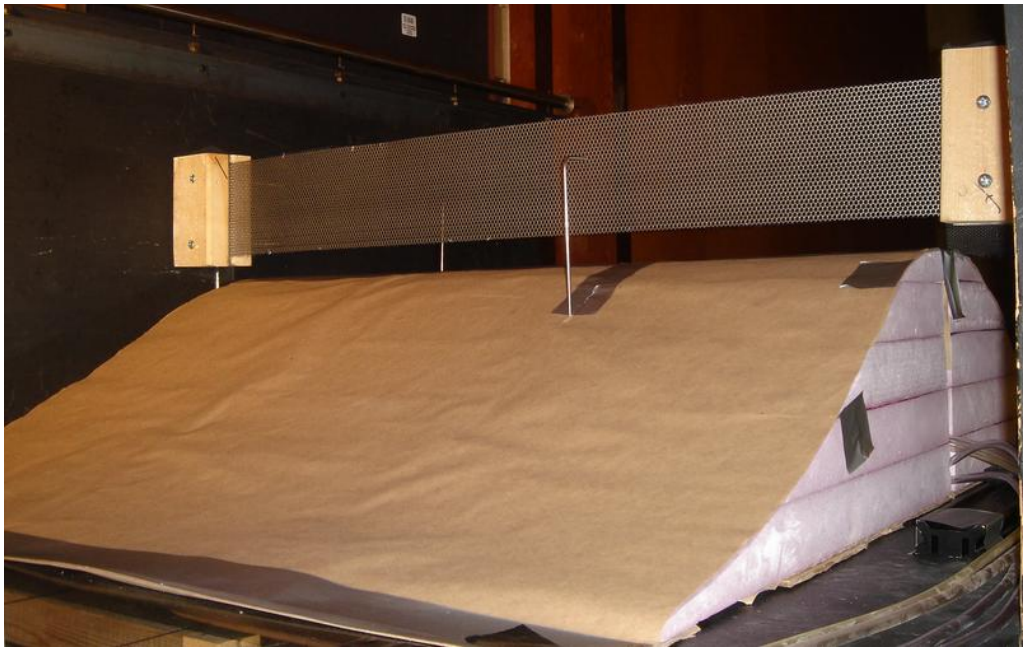

Figure 28: Surface design and perforated plate testing set-up with pitot tubes.

It can be observed from Figure 28 that there is a pitot tube on each side of the perforated plate facing the oncoming airflow. The actual fabricated shape can be seen, as well as the final perforated plate with the correct size and porosity.

After velocity and pressure data was taken for the shape and plate, it had to be analyzed thoroughly to understand how the shape would affect power output of a mounted wind turbine. In fluid flow the power is related to the pressure difference, flow speed and area through which the fluid is flowing is given as

$$P = \Delta pVA$$

Where Δp is the pressure difference, V is the flow speed and A is the area through which the fluid is flowing. Using the mesh cross sectional area as A, the velocity measured at the upstream pitot tube as V and the pressure difference measured between the two pitot tubes as the Δp, the theoretical power output to the mesh (idealized as an model turbine) can be estimated. Data was taken with the mesh at 1 inch above the centerline of the shape and at various locations downstream of the shape centerline. Those locations were 0 inches, 0.75 inches, 1 inch, and 5 inches. A schematic of different locations is shown below in Figure 29. Data was also taken with just the mesh and no shape as a base line but this is not shown in Figure 29.

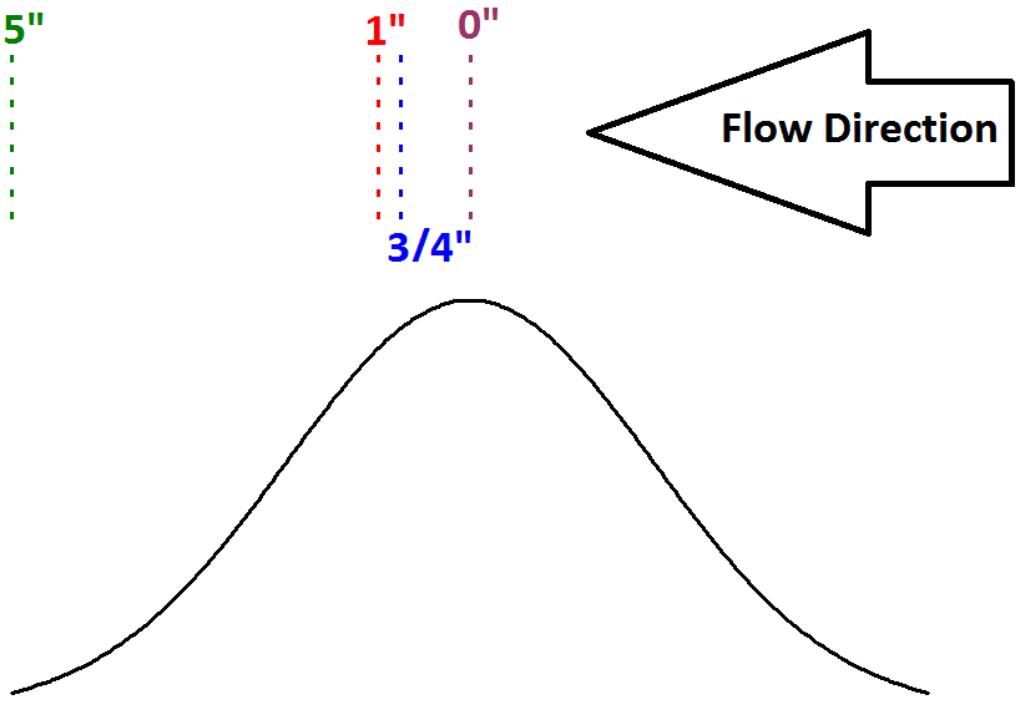

Figure 29: Schematic of mesh at different locations downstream from the shape centerline

The Δp was determined for the different flow speeds by first converting the manometer readings which were in mm WC to Pa, then multiplying the value by two due to the fact that the manometer only takes one half of pressure drop into account . The flow velocity was then determined at the upstream pitot tube using the pressure transducer. The velocity through the mesh was approximated to be this upstream pitot tube location. The area of the mesh, A, was simply determined to be 0.155 m^2. Using this data a theoretical power output versus velocity was constructed and is shown below in Figure 30. Note that this approximates what the power output would be for a wind turbine with a similar cross sectional area, *A*.

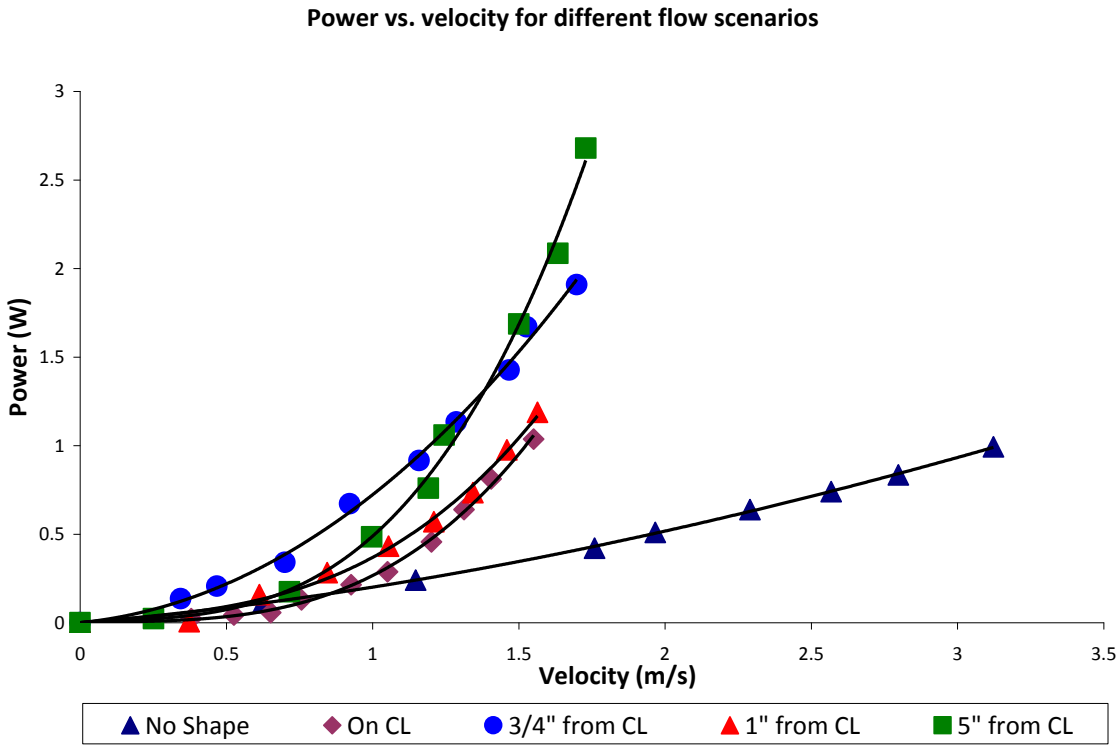

Figure 30: Theoretical power output vs. velocity

Using Microsoft Excel's fitting tools each data set was fit to a 3rd degree polynomial each with a R^2 value (a goodness-of-fit indicator) above 99% which is good because power varies with velocity cubed (which is not indicated directly in the power equation shown above). Using these fits values for the power output for the mesh with no shape with the mesh at different locations relative to the centerline for a flow speed of 1.5 m/s were determined for comparison purposes. A plot of this information is shown below in Figure 31.

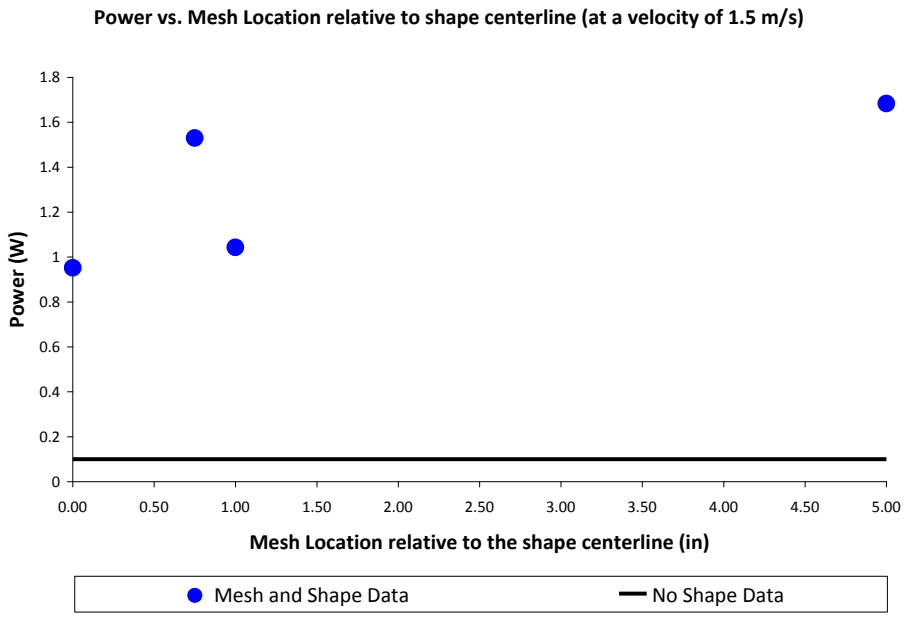

Figure 11: Power vs. Mesh location downstream from shape CL and power from no shape case

From Figures 30 and 31 the data is showing quite clearly that the theoretical power output for the mesh is higher than the case with no shape. The velocity values do not reach as high in the cases with the shape as they do with the no shape cases, but the pressure drop values are much higher. This higher pressure drops with the shape lead to the higher power outputs. Moving the mesh relative to the shape centerline has an effect on the power output. The highest power output occurred when the mesh was 5" downstream of the shape centerline. As you get closer to the shape centerline the power output seems to decrease except at 0.75" which may be an outlier (more testing would clarify this). The difference in power output at 1.5 m/s for when the mesh is 5" from the centerline of the shape and for when there is no shape is 178%. These tests should be run again in later IPROs to verify and expand upon this information.

Appendix J
Architectural Findings

A major task for the architecture team was to come up with estimations of how much it would cost to implement these structures onto urban buildings. After some research, estimated prices for fabricating one surface mount structure with a wind turbine are as follows:
Wind power has become increasingly popular in recent years and wind farms are sprouting up all over rural America. However, power is used predominantly in cities, and transmission loss is serious between the open plains states and the eastern seaboard. Traditional thinking in wind power depends on broad open spaces with steady flows. For better application in the variable winds of the urban environment a system must have the capacity to change with the changing wind orguide and direct the wind to a stationary turbine.

Through the course of the semester development from an architectural standpoint has happened in the background. One focus was determining the scale and possible applications of the modules. This involved modeling of a mock tunnel and towers, determining potential outputs and designing the structure of the individual units.

A shape prototype was designed by the engineers. To produce useful energy, many of these structures must be implemented on the same building just as many horizontal axis wind turbines are installed in fields of wind farms. Some three-dimensional architectural renderings were created to visualize the surface of a building with the surface structure and possible wind turbines installed:

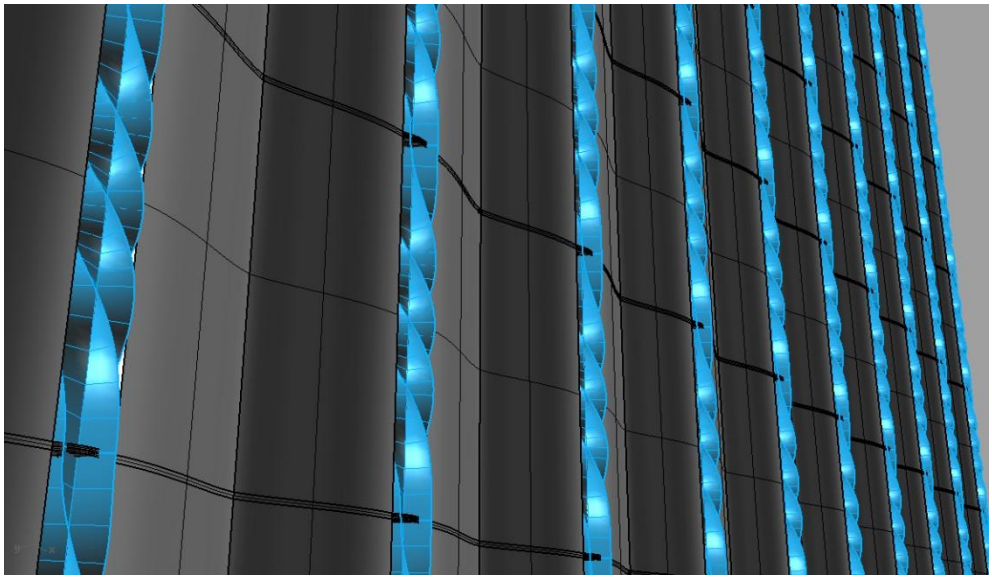

Figure 32: Surface design with helical turbines located at the center of each shape.

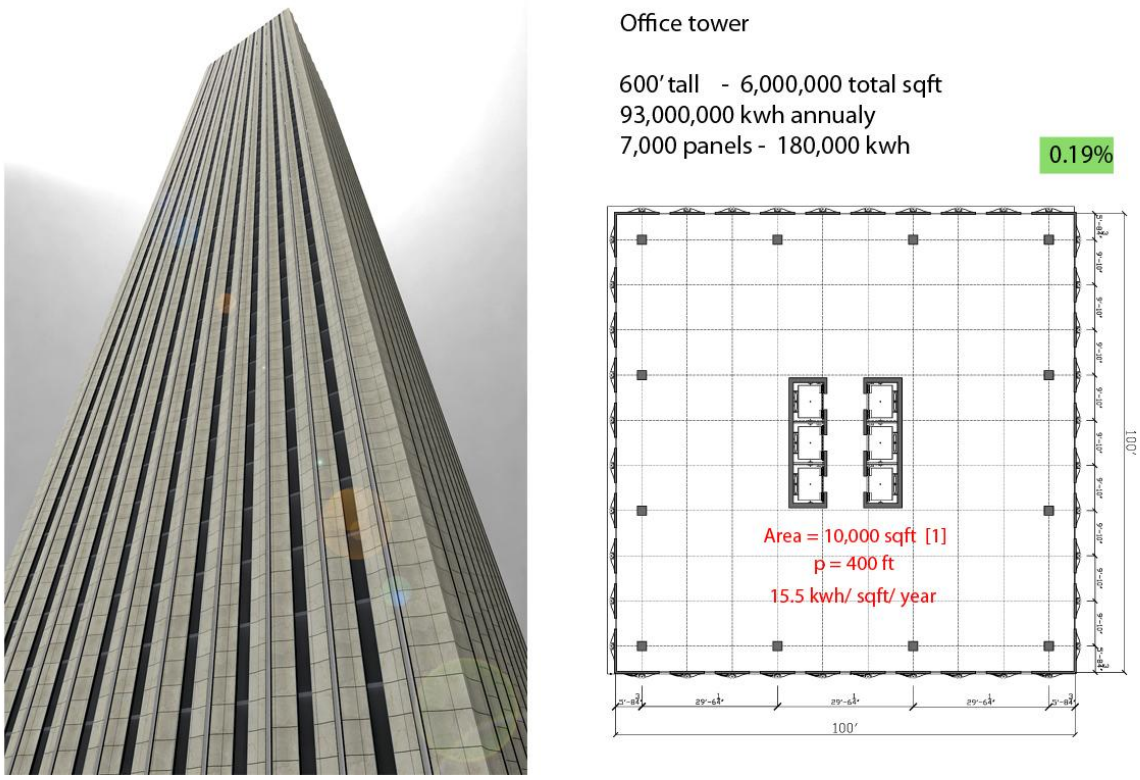

Figure 33: Example of a high-rise building with the surface design implemented vertically along the sides of the building.

Figure 34: Example of shorter buildings with the surface shape designed to cover the roof.

An analysis of the surface area of building sides, sizing and spacing was done to determine the most efficient architectural set-up for the wind turbine modules:

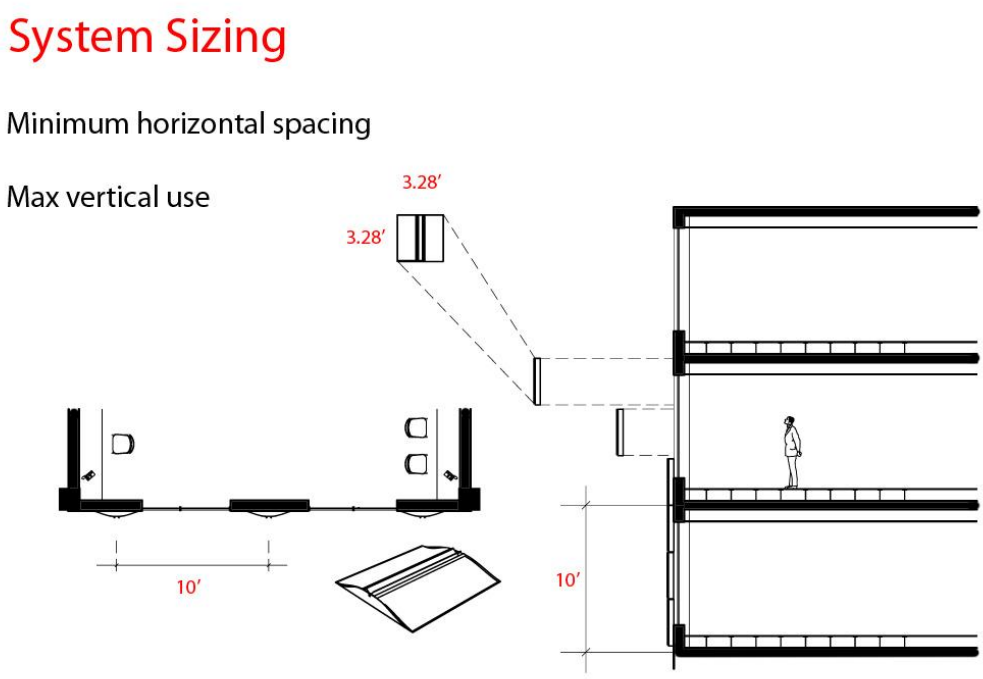

Figure 35: A schematic of a building with the wind turbine surface design integrated onto the side.

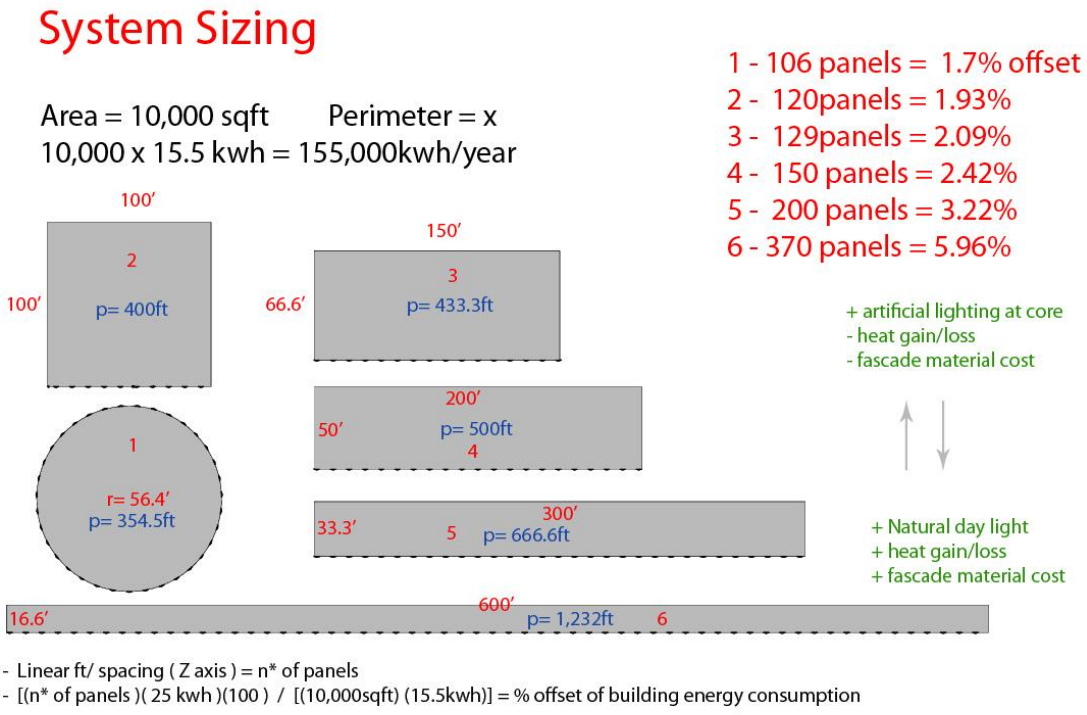

Figure 36: An example of buildings with the same area and different perimeters.

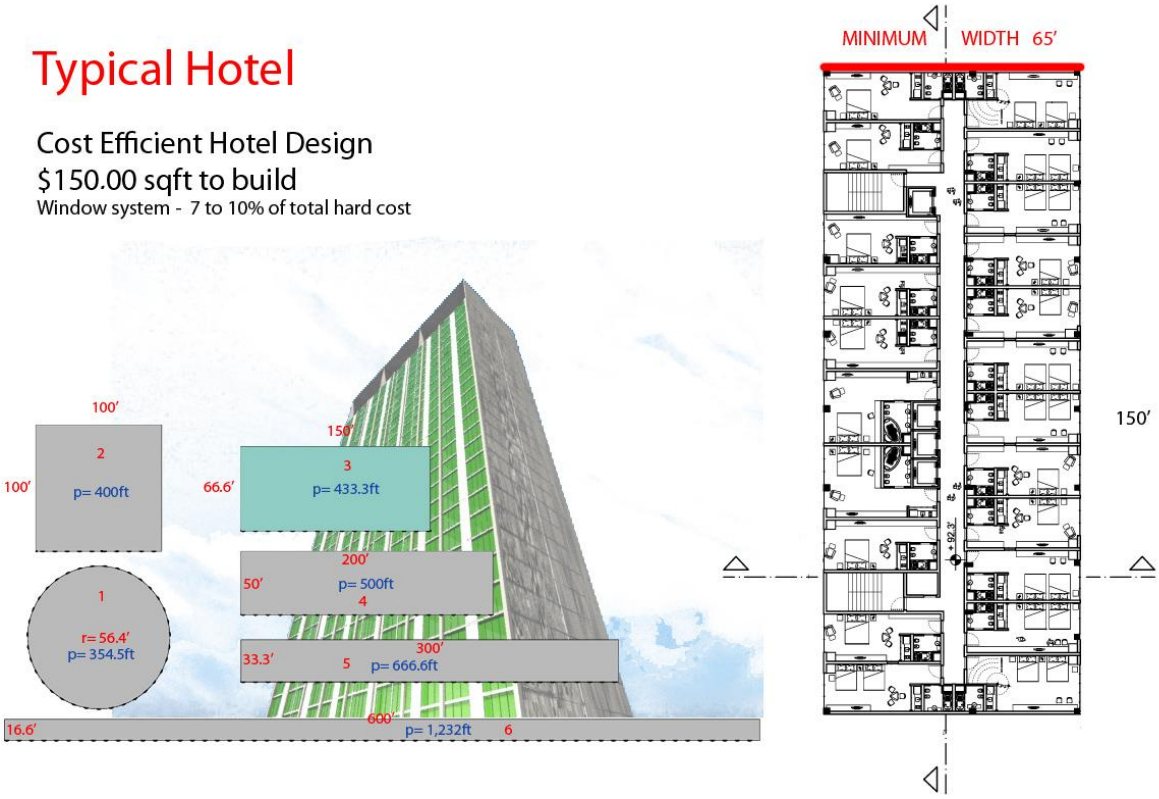

Figure 37: Analysis of hotel design and building perimeter.

Power consumption of typical urban buildings was researched and a list is located in Appendix D.These values are important in architectural analysis to consider the percentage of power a series of surface mount wind turbines would produce for a typical urban building.

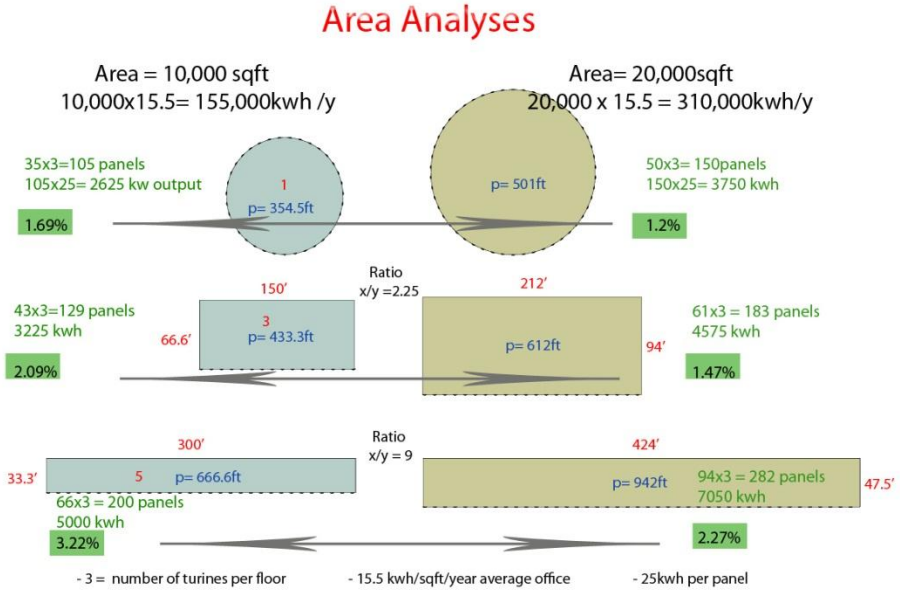

Figure 38: Analysis of power consumption for different sized buildings.

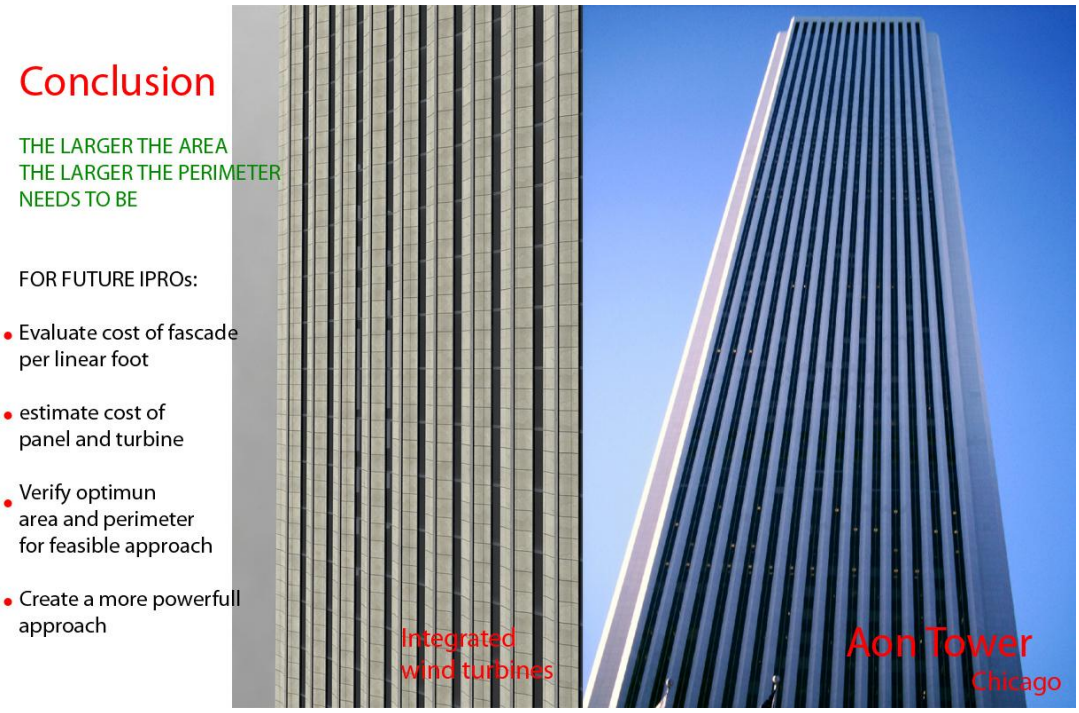

Figure 39: Recommendations for future architectural research in IPRO 323.

Another aspect the architectural research team had to consider was the power output at different wind speeds, and the average wind speeds in Chicago at different building heights. Calculations were made using the data gathered for the current surface design prototype and an ideal wind turbine, assuming that the ideal Betz' limit of 59.3% of the wind power was extracted and used by the turbines, and that the air density is 1.225 kg/m^3. The area used for the calculations was 0.137 m^2, which was the area of the perforated plate tested. The calculated values are as follows:

Wind Speed (m/s)	Wind Speed (mi/hr)	Annual Power (kW-hr/m^2)	Annual Power (kW-hr)
5	11.2	398	54.53
10	22.4	3182	435.9
15	33.6	10,740	1471

Table 4: Annual power output for increasing wind speeds typical of urban environments.

Another major task for the architecture team was to come up with estimations of how much it would cost to implement these structures onto urban buildings. After some research, estimated prices for fabricating one surface mount structure with a wind turbine are as follows:

- Tubular aluminum frame
  - Approx. 45' of ¾" sq. tubing $50
  - Welded $15
- Molded plastic upper $5

- Turbine body
  - Solid paddle $10
  - Solid savonious $20
  - Membrane paddle/savonious $30
- Magnetic generator $100
- Transformer $70
- Total $300

This cost estimates the price of only one component being implemented on a building; however, to produce useful energy, many of these structures must be implemented on the same building just as many horizontal axis wind turbines are installed in fields of wind farms.